

1999

Synthesis of octa-tailed calix[4]resorcinarenes and characterization of Langmuir-Blodgett films on these compounds.

Yong Chun. Chen
University of Windsor

Follow this and additional works at: <http://scholar.uwindsor.ca/etd>

Recommended Citation

Chen, Yong Chun., "Synthesis of octa-tailed calix[4]resorcinarenes and characterization of Langmuir-Blodgett films on these compounds." (1999). *Electronic Theses and Dissertations*. Paper 3702.

This online database contains the full-text of PhD dissertations and Masters' theses of University of Windsor students from 1954 forward. These documents are made available for personal study and research purposes only, in accordance with the Canadian Copyright Act and the Creative Commons license—CC BY-NC-ND (Attribution, Non-Commercial, No Derivative Works). Under this license, works must always be attributed to the copyright holder (original author), cannot be used for any commercial purposes, and may not be altered. Any other use would require the permission of the copyright holder. Students may inquire about withdrawing their dissertation and/or thesis from this database. For additional inquiries, please contact the repository administrator via email (scholarship@uwindsor.ca) or by telephone at 519-253-3000ext. 3208.

INFORMATION TO USERS

This manuscript has been reproduced from the microfilm master. UMI films the text directly from the original or copy submitted. Thus, some thesis and dissertation copies are in typewriter face, while others may be from any type of computer printer.

The quality of this reproduction is dependent upon the quality of the copy submitted. Broken or indistinct print, colored or poor quality illustrations and photographs, print bleedthrough, substandard margins, and improper alignment can adversely affect reproduction.

In the unlikely event that the author did not send UMI a complete manuscript and there are missing pages, these will be noted. Also, if unauthorized copyright material had to be removed, a note will indicate the deletion.

Oversize materials (e.g., maps, drawings, charts) are reproduced by sectioning the original, beginning at the upper left-hand corner and continuing from left to right in equal sections with small overlaps.

Photographs included in the original manuscript have been reproduced xerographically in this copy. Higher quality 6" x 9" black and white photographic prints are available for any photographs or illustrations appearing in this copy for an additional charge. Contact UMI directly to order.

Bell & Howell Information and Learning
300 North Zeeb Road, Ann Arbor, MI 48106-1346 USA
800-521-0600

UMI[®]

**SYNTHESIS OF OCTA-TAILED CALIX[4]RESORCINARENES AND
CHARACTERIZATION OF LANGMUIR-BLODGETT FILMS OF THESE
COMPOUNDS**

by

Yong Chun Chen

A Dissertation Submitted to the Faculty of Graduate Studies and Research through the
Department of Chemistry and Biochemistry in Partial Fulfillment of the Requirements for
the Degree of Masters of Science at the University of Windsor

Windsor, Ontario, Canada

May 1999



National Library
of Canada

Bibliothèque nationale
du Canada

Acquisitions and
Bibliographic Services

Acquisitions et
services bibliographiques

395 Wellington Street
Ottawa ON K1A 0N4
Canada

395, rue Wellington
Ottawa ON K1A 0N4
Canada

Your file *Votre référence*

Our file *Notre référence*

The author has granted a non-exclusive licence allowing the National Library of Canada to reproduce, loan, distribute or sell copies of this thesis in microform, paper or electronic formats.

L'auteur a accordé une licence non exclusive permettant à la Bibliothèque nationale du Canada de reproduire, prêter, distribuer ou vendre des copies de cette thèse sous la forme de microfiche/film, de reproduction sur papier ou sur format électronique.

The author retains ownership of the copyright in this thesis. Neither the thesis nor substantial extracts from it may be printed or otherwise reproduced without the author's permission.

L'auteur conserve la propriété du droit d'auteur qui protège cette thèse. Ni la thèse ni des extraits substantiels de celle-ci ne doivent être imprimés ou autrement reproduits sans son autorisation.

0-612-52742-5

Canada

Abstract

This project was focused on synthesis of octa-tailed calix[4]resorcinarenes functionalized with pendant α -(diethyl acetamide) or α -(methyl acetate), preparation of Langmuir films and Langmuir-Blodgett films of the calix[4]resorcinarenes, and characterization of these compounds in solution and the Langmuir-Blodgett films.

The history of the supramolecular chemistry including preparation and conformation of tetra-tailed calix[4]arene and calix[4]resorcinarene is reviewed. The physical properties of Langmuir films and Langmuir-Blodgett films are also introduced. The strategy of this project was to develop the synthesis of octa-tailed calix[4]resorcinarenes functionalized with pendant α -(diethyl acetamide) or α -(methyl acetate), to prepare and characterize Langmuir films and Langmuir-Blodgett films of the resorcinarenes.

The octa-tailed calix[4]resorcinarene was synthesized by the cyclooligomerization of resorcinol and α,α -dihexyl acetaldehyde under acid-catalyzed conditions. The α,α -dihexyl acetaldehyde was made through the reaction of dihexyl ketone with a phosphonate reagent. Subsequently, the functionalized octa-tailed calix[4]resorcinarenes were obtained by substitution reaction with 2-bromo-*N,N*-diethyl acetamide or methyl bromoacetate under basic conditions.

The flattened cone conformation was identified in the free functionalized resorcin[4]arene and its complex with silver ion in solution by variable temperature ^1H NMR studies. The free energies of activation were determined from the coalescence

temperature for the pseudorotation of the free functionalized octa-tailed resorcin[4]arene and the functionalized octa-tailed resorcin[4]arene bound with silver ion in solution.

Langmuir films of the octa-tailed resorcin[4]arenes and their amide and ester derivatives were fabricated at the air/water interface. The π - A isotherms were found to vary as a result of changing spreading solvent, subphase temperature and structure modification in the resorcin[4]arene tail section. One-layer LB film of the octa-tailed resorcinarene amide derivative incorporated with Ag^+ and ten-layer LB film of the octa-tailed resorcinarene ester derivative incorporated with Ag^+ were fabricated on quartz. Both the cone and flattened cone conformations could be seen in the UV-visible spectra of LB films of the octa-tailed resorcin[4]arene amide or ester derivatives.

Acknowledgment

I am greatly indebted to my advisor, Dr. Philip Dutton, for financial assistance, academic guidance and understanding throughout my research program.

I also wish to express my thanks to all faculty members, graduate students and staff in the department for their help, but I would like to particularly mention my lab mates, Jay and Kevin McKay, with whom I had the pleasure of sharing time and many discussions. Thanks also to Dr. John McIntosh and Dr. Jim Green for their academic help.

My parents and my wife have always been a support to my work. Especially I would appreciate my son, Patrick, born in the second year of my graduate studies for his inspiration.

Table of Contents

Abstract.....	III
Acknowledgments.....	V
List of Tables	VIII
List of Figures	IX
List of Abbreviations	XII
1. Introduction.....	1
1.1. Introduction of Supramolecular Chemistry	1
1.1.1 Introduction.....	1
1.1.2. Macrocyclic Molecules.....	2
1.1.2.1 Crown Ethers	2
1.1.2.2 Cryptands	4
1.1.2.3 Spherands.....	5
1.1.3 Self-Organized Molecules	6
1.1.4 Applications	9
1.2. Calixarene and Calixresorcinarene Chemistry	9
1.2.1 Historical Introduction of Calixarenes and Calixresorcinarenes	10
1.2.2 The Syntheses of Calixarenes and Calixresorcinarenes.....	14
1.2.3 Conformations of Calix[4]arenes and Calix[4]resorcinarenes	16
1.2.4 Functionalized Calix[4]resorcinarenes	20
1.2.5 Calix[4]resorcinarenes as Host Molecules.....	23
1.3. Langmuir-Blodgett Films.....	26
1.3.1. Formation of Langmuir Films and Langmuir-Blodgett Films	26

1.3.1.1 Surface Pressure/Area Isotherms	26
1.3.1.2 Langmuir-Blodgett Deposition	29
1.3.2. Types of Molecules to Form Langmuir Films and Langmuir-Blodgett Films	30
1.3.2.1 Fatty Acids and Derivatives.....	30
1.3.2.2 Aromatic Hydrocarbons and Derivatives.....	32
1.4 Objective	34
2. Results and Discussion	37
2.1. Synthesis..	37
2.1.1 α,α -Dihexyl Acetaldehyde	37
2.1.2 Octa-Tailed Calix[4]resorcinarenes	42
2.1.3 Octa-Functionalized the Calix[4]resorcinarenes.....	45
2.2 Characterization in Solution	51
2.3. Behavior of Langmuir-Blodgett Films.....	58
2.3.1 Langmuir Film Properties	59
2.3.2 The Characteristics of Langmuir-Blodgett Films..	66
2.4 Characterization in Langmuir-Blodgett Films	69
2.5 Conclusion	72
3. Experimental	74
3.1 General Procedures and Instruments	74
3.2 Materials	74
3.3 Preparation of Langmuir Films and Langmuir-Blodgett Films	86
4. References.....	87
Vita Auctoris.....	93

List of Tables

Table 1	The different types of surfactants	7
Table 2	Complexation-induced ^1H NMR shifts (CIS).....	24
Table 3	The data of ^1H NMR of 21 and 22.....	43
Table 4	The data of ^1H NMR of 25 - 29	50
Table 5	The free energy of activation of 26 and the coalescence temperature	56
Table 6	The limiting area and collapse pressure of 21 - 29 from 10% MeOH/ CHCl_3 at 25°C	64

List of Figures

Figure 1	Scheme of formation of supramolecule from single molecules	3
Figure 2	Examples of metal ions bound within crown ethers.....	4
Figure 3	Examples of bicyclic cryptands.....	6
Figure 4	Examples of spherands	7
Figure 5	Accumulation and orientation of surfactant molecules at interface	8
Figure 6	Cross section of idealized spherical micelle with positive counter ions	8
Figure 7	Typical structures of calix[4]arene and calix[4]resorcinarene	10
Figure 8	Lederer and Manasse's reaction.....	11
Figure 9	Structure of Neiderl's octols	12
Figure 10	Zinke and Ziegler's <i>p</i> - <i>tert</i> -butylphenol cyclic tetramer	13
Figure 11	Zinke-Cornforth-Gutshe's procedure.....	15
Figure 12	Neiderl-Högberg procedure.....	15
Figure 13	Calix[4]arene conformations	17
Figure 14	X-ray crystallographic structure of <i>p</i> - <i>tert</i> -butylcalix[4]arene in the cone conformation	17
Figure 15	X-ray crystallographic structure of Högberg-Nilsson's <i>C</i> - <i>p</i> - bromophenylcalix[4]resocinarene.....	18
Figure 16	Calix[4]resorcinarene conformations	19
Figure 17	"Upper rim" bridged calix[4]resorcinarenes.....	21
Figure 18	Structure of a carcerand.....	22

Figure 19	Hydrogen bonding at proximate OH groups of Calix[4]resorcinarene	23
Figure 20	Bound silver ion within the cavity.....	25
Figure 21	Surface pressure-area isotherm of stearic acid on water subphase.....	27
Figure 22	Monolayer of stearic acid on water surface: (a) expanded, (b) partly compressed, (c) close packed.....	28
Figure 23	Collapse of Langmuir film	28
Figure 24	Deposition of multilayers by the LB technique: (a) first immersion, (b) first withdrawal, (c) second immersion, (d), second withdrawal.....	29
Figure 25	Structures of X, Y, and Z type depositions	30
Figure 26	Surface pressure-area isotherm of oleic epoxide.....	31
Figure 27	Surface pressure-area isotherm of (8) _n	33
Figure 28	Scheme of the selective formation of the (8) ₄ /Na ⁺ complex at the air/water interface	33
Figure 29	Theoretical head and tail sizes of four-tailed resorcin[4]arene and eight-tailed resorcin[4]arene	35
Figure 30	Synthesis of α,α -dihexyl acetaldehyde	37
Figure 31	¹ H NMR spectrum of 20.....	39
Figure 32	¹³ C NMR spectrum of 20.....	40
Figure 33	MS spectra of (a) pure 20 and (b) oxidized 20.....	41
Figure 34	Synthesis of calix[4]resorcinarenes	42
Figure 35	MS spectrum of 21	44
Figure 36	MS spectrum of 22	45
Figure 37	Synthesis of 2-bromo- <i>N,N</i> -diethylacetamide	46

Figure 38	Synthesis of octa-functionalized calix[4]resocinarenes	47
Figure 39	Pseudorotation of flattened cone conformation.....	48
Figure 40	¹ H NMR spectrum of 26.....	49
Figure 41	Variable temperature ¹ H NMR spectra of aromatic region of 26 in CD ₂ Cl ₂	53
Figure 42	Variable temperature ¹ H NMR spectra of non-aromatic region of 26 in CD ₂ Cl ₂	54
Figure 43	The arene rings and their protons in the flattened cone conformation	55
Figure 44	Comparison of ¹ H NMR spectra of arene region of 26 and 26•Ag ⁺ in CD ₂ Cl ₂	57
Figure 45	Variable temperature ¹ H NMR spectra of aromatic region of 26•Ag ⁺ in CD ₂ Cl ₂	58
Figure 46	Surface pressure-area isotherm of 22 at 15°C	61
Figure 47	Surface pressure-area isotherm of 22 at 25°C	62
Figure 48	Surface pressure-area isotherm of 21 from 10% MeOH/CHCl ₃	62
Figure 49	Surface pressure-area isotherm of 21 from toluene.....	63
Figure 50	UV-visible spectra of 01 LB of (a) 26 and (b) 26•Ag ⁺	69
Figure 51	UV-visible spectra of 01 LB of (a) 29 and (b) 29•Ag ⁺ and (c) 10 LB 29•Ag ⁺	71

List of Abbreviations

A	limiting area (π -A isotherm)
br	broad (IR)
Bu	butyl
°C	degrees Celsius
δ	chemical shift
ΔG^\ddagger	free energies of activation at coalescence temperature
cal	calorie
cm	centimetres
cm^{-1}	wavenumbers
CPK	Corey-Pauling-Koltun
DHP	dihydropyran
Et	ethyl
EtOH	ethanol
Et ₂ O	diethyl ether
g	grams
h	Plank's constant
h	hour
IR	infrared
k	kilo
K	kelvin
k_B	Boltzmann's constant

k_c	exchange rate at coalescence temperature
λ	wave length
m	metres, multiplet (NMR)
<i>m</i>	meta
M	molarity
Me	methyl
MHz	megaHertz
min	minutes
mmHg	millimetres of mercury
mL	millilitres
mmol	millimoles
mp	melting point
nm	nanometres
NMR	nuclear magnetic resonance
<i>o</i>	ortho
<i>p</i>	para
Ph ₂ O	diphenyl ether
ppm	parts per million
q	quartet (NMR)
s	strong (IR), singlet (NMR)
t	triplet (NMR)
<i>t</i>	tert
T_c	coalescence absolute temperature

THF	tetrahydrofuran
THP	tetrahydropyran
TLC	thin layer chromatography
UV-vis	ultra-violet visible spectrometry
vs	very strong (IR)
w	weak (IR)
Y	yield

1. INTRODUCTION

1.1. Introduction of Supramolecular Chemistry

1.1.1 Introduction

Supramolecular chemistry is a relatively young field. There has not been a formal structure given in this field. Strictly, supramolecular chemistry is associated with molecules and their intermolecular interactions.¹

In contrast to molecular chemistry, which is predominately based on the covalent bonding of atoms, supramolecular chemistry is based on non-covalent, multiple intermolecular interactions between a least two building blocks. The formation of such a supramolecule, which is contrasted with that of a single molecule, is schematically shown in Figure 1.¹ The intermolecular interactions include electrostatic forces, hydrogen bonding, and van der Waals forces. In a defined structural system, the molecules designated as “receptor” or “host” bind “substrate” or “guest” strongly and selectively by forming supramolecular structures or supramolecules. The receptor molecule is usually defined as the larger molecule compared to the substrate.² The receptor molecule recognizes the substrate molecule by providing a two or three dimensional shape which complements the substrate’s shape. In order to complex, the receptor molecule binding sites must converge on the substrate in the complex, and the substrate molecule must have binding sites that diverge in the complex.³

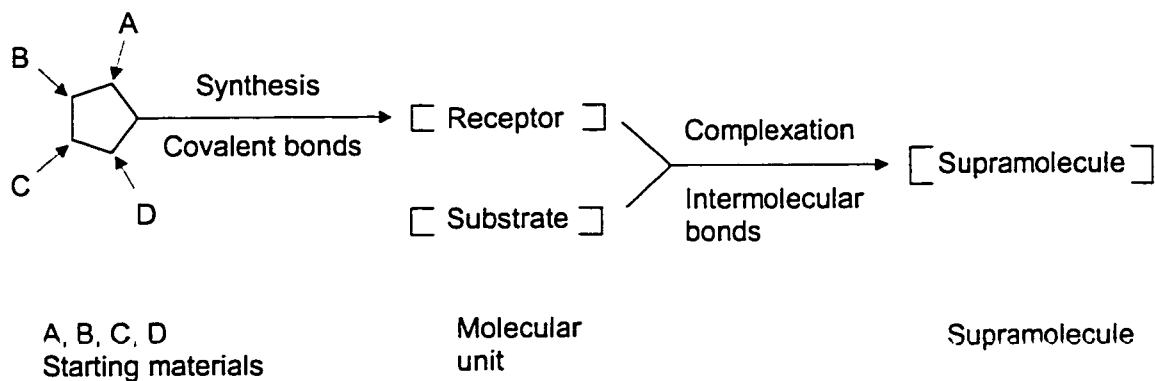


Figure 1. Scheme of formation of supramolecule from single molecules.¹

1.1.2. Macrocyclic Molecules

Supramolecular chemistry is based both on the development of the chemistry of crown ethers and cryptands, and on the progress made in the study of the self-organization of molecules.⁴

The crown ethers were first discovered and studied 30 years ago by C. J. Pedersen,⁵ and materials called cryptands and spherands were initially introduced by J.-M. Lehn⁶ in 1969 and D. J. Cram⁷ in 1974, respectively. In 1987, Pedersen, Lehn and Cram shared the Nobel Prize for their important contributions to supramolecular chemistry.^{3,8,9}

1.1.2.1 Crown Ethers

The serendipitous discovery of crown ethers has fundamentally given new impulses to the chemistry of complexes with organic ligands, especially neutral ones.⁴

Pedersen discovered the ability of crown ethers to selectively bind alkali metals in rigid and structured complexes. The selective binding was dependent upon the size of the macrocyclic ring.^{5,10} Figure 2 is an example of an 18-crown-6 compound binding K^+ in contrast to 12-crown-4 compound which binds Li^+ but not K^+ . The positively charged metal ions were tightly held in the center of the oxygen atoms with electrostatic forces such as ion-dipole interactions. Such macrocyclic effect is of two-dimensional intermolecular interactions with multi-binding sites and exhibits stronger binding ability than chelate effect that is of one-dimensional intermolecular interactions with single binding site.⁸

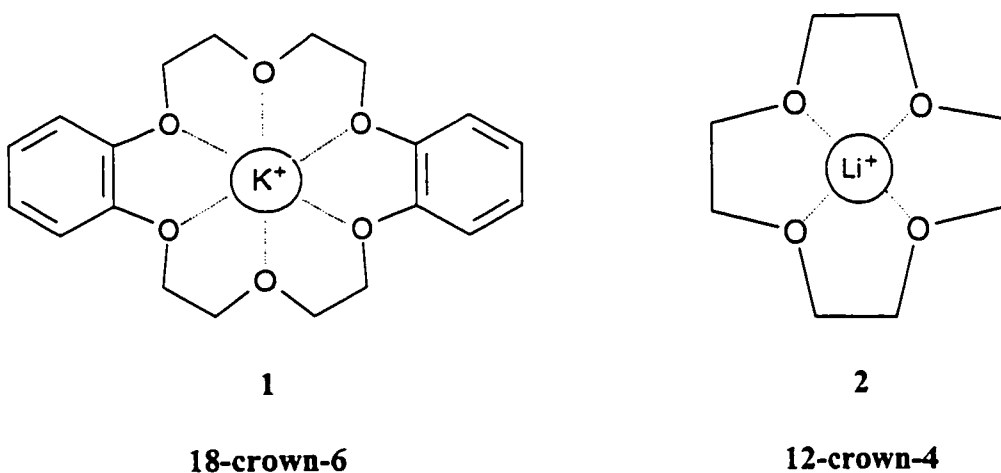


Figure 2. Examples of metal ions bound within crown ethers.

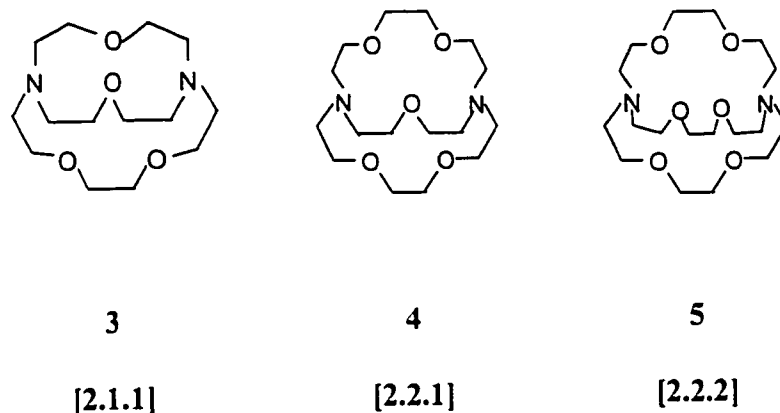


Figure 3. Examples of bicyclic cryptands.

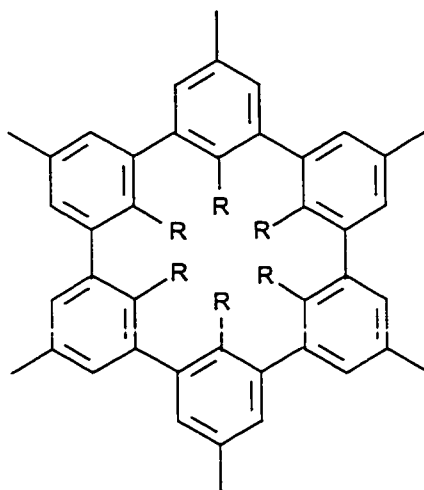
1.1.2.2 Cryptands

Bicyclics and cycles of higher order are called cryptands, and the complexes formed are called cryptates. Lehn developed these kinds of compounds.¹¹ Examples of the bicyclic cryptands are shown in Figure 3. The notation commonly used for these compounds consists of a series of numbers in square brackets, each representing the number of the donor sites in each of the bridges. The cryptands have a three dimensional cavity, which varies in size as the lengths of the bridges that contain the donor sites are varied. The spherical recognition to substrate was defined as cryptate effect.¹ The cryptate effect is a more effective intermolecular interaction than the macrocyclic effect since cryptands with spherical cavity are found more compatible to complex with spherical cations than two-dimensional crown ethers.¹ The cryptate effect was characterized by high stability and selectivity, low exchange rates, and efficient shielding

of the bound ion from the environment.³ Variation in the length of the glycol bridges was found to alter the selectivity for different alkali metals.¹ The [2,1,1] cryptand selectively bound lithium ion, the [2,2,1] cryptand bound sodium ion, and the [2,2,2] cryptand was found to be selective for potassium ion.

1.1.2.3 Spherands

A series of new compounds in Figure 4, known as spherands, were made and studied by D. J. Cram.^{12,13} The spherands contain the donor centers (OCH₃, OH, O⁻) as intraannular substituents which point into the interior of a rigid ring. From the investigation of the peregrinated spherands binding alkali cations, Cram proposed the principles of preorganization and complementary for forming supramolecules.^{3,13} The preorganization indicates a strong binding between the receptor molecule called host and the substrate called guest benefits from small changes in the organization of a) the host, b) the guest and c) the solvent required for complexation. The complementary principle states that in order to complex, the host must have binding sites that cooperatively contact and attract the binding sites of the guest without the generation of strong non-bonding repulsion.



6, R = OCH₃
 7, R = OH
 8, R = O⁻

Figure 4. Examples of spherands.

1.1.3. Self-Organized Molecules

The study of the self-organization of molecules such as surfactants and membrane is also an important part in supramolecular chemistry. Surfactants (surface-active agents) are compounds containing both non-polar and polar groups. The non-polar (hydrophobic) groups are generally prepared from hydrocarbon chains and aromatics. The surfactants can be divided into anionic, cationic, amphoteric and non-ionic categories, according to the types of polar groups, as given in Table 1.¹⁴

Table 1. The different types of surfactants.

Structure	Designation	Type
$\text{CH}_3(\text{CH}_2)_{16}\text{COONa}$	Sodium stearate	Anionic
$\text{RN}^+(\text{CH}_3)_3\text{Cl}^-$	Quaternary ammonium salts	Cationic
$\text{RCHN}^+(\text{CH}_3)_3\text{COO}^-$	Betaines	Amphoteric
$\text{RO}(\text{CH}_2\text{CH}_2\text{O})_n\text{H}$	Fatty acid polyglycol esters	Non-ionic

* R = mostly long-chain alkyls

As result of the hydrophobic and hydrophilic groups, the surfactant molecules are preorganized at interfaces of dissimilar media such as water/air. In water the hydrophilic groups are extended into the aqueous phase, while the hydrophobic chains are squeezed out of it. Thus, the surfactants are found at the water/air interface to form a monomolecular layer, as shown in Figure 5.¹⁵ The layers can be applied in numbers and orientation on a support. For example, Langmuir-Blodgett film was fabricated on glass slide from water/air interface by the dipping method. Moreover, when the surfactant molecules are added to the surface layer the surface tension usually decreases because the attractive forces of hydrophobic hydrocarbon chains are considerably weaker compared to water. This “surface activation” is used in washing, rinsing, and cleaning processes and cosmetic and pharmaceutical industries.

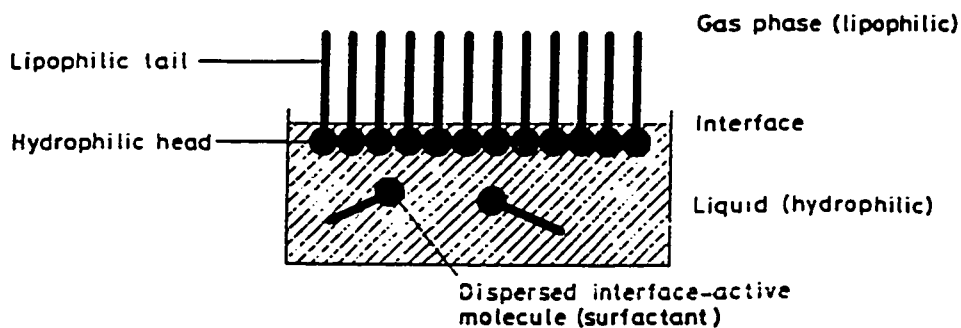


Figure 5. Accumulation and orientation of surfactant molecules at interface.¹⁴

Micelles are formed in a special form of surfactant aggregation, in which dissolved surfactant molecules react to the repelling action of surrounding water. An idealized spherical anionic micelle with positive counter ions is shown in Figure 6.¹⁴ The hydrophobic groups of the surfactant molecules are gathered at the center of the spherical droplet, while the hydrophilic groups are pointing outwards. Therefore, micelle solution represents micro-heterogeneous media.

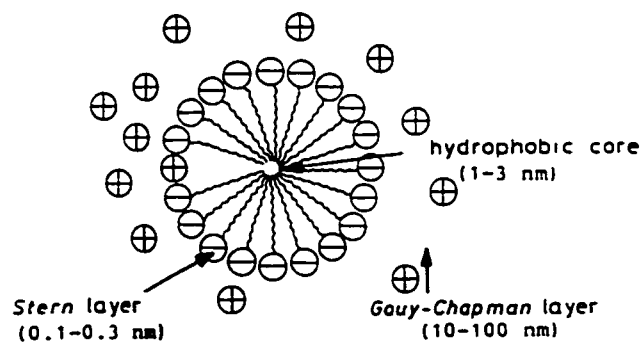


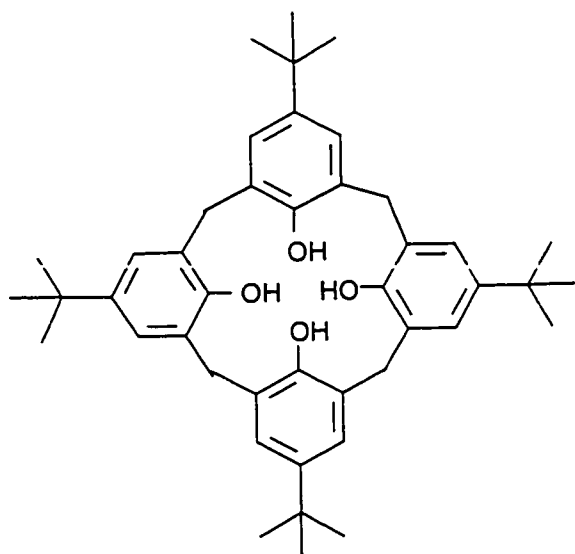
Figure 6. Cross section of idealized spherical micelle with positive counter ions.¹⁴

1.1.4 Applications

In the field of supramolecular chemistry, the macrocyclic materials as acceptor or host and self-organized molecules are of great industrial and economic interest. The applications of these materials include molecular sensors, bioorganic model compounds, liquid crystals, surfactants, organic semi-conductors, conductors, superconductors and molecular wires.⁴

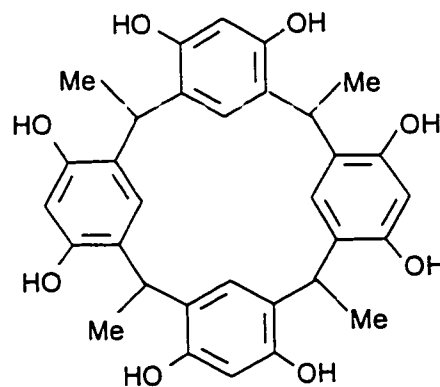
1.2. Calixarene and Calixresorcinarene Chemistry

Although the calixarene and calixresorcinarene field of chemistry is a relatively old one, as host molecules, calixarene and calixresorcinarene have recently received considerable attention. The name calixarene refers to the bowl- or chalice-like shape of compounds such as *p*-*tert*-butylcalix[4]arene, **9** (Figure 7). The calixarenes are macrocyclic compounds comprising four or more phenolic moieties joined in cyclic array at the *meta*-positions by methylene groups. The bracketed number representing the number of aryl groups in these oligomers is inserted between calix- and -arene. The *p*-substituent is designated to the calixarene derived from starting phenol. The calixresorcinarenes are resorcinol-derived calixarenes such as *C*-methylcalix[4]resorcinarene (**10**). The bracketed number is inserted between the calix- and -resorcinarene. The substituent, which is introduced by the starting aldehyde at the methylene carbons, is indicated by a prefix “*C*-substituent”. Recently, the calix[4]resorcinarenes are also abbreviated as “resorcin[4]arenes” in some publications.¹⁶



9

p-tert-Butylcalix[4]arene



10

C-Methylcalix[4]resorcinarene

Figure 7. Structures of calix[4]arenes and calix[4]resorcinarenes.

1.2.1 Historical Introduction of Calixarenes and Calixresorcinarenes

Calixarene chemistry began over a century ago when Adolph von Baeyer¹⁷ studied the reactions of aldehydes and phenols in the presence of strong acids. The reaction between benzaldehyde and benzene-1,2,3-triol under acidic conditions was found to give a red-brown, resin-like product. Like other aldehydes, formaldehyde condensed with phenol, in the presence of a mineral acid, producing resins. Because of the inability

to obtain these compounds in a pure form, Baeyer did not characterize them with elemental analysis, thus possible structures were not proposed.¹⁸

L. Lederer¹⁹ and O. Manasse²⁰ independently studied the reaction between formaldehyde and phenol under basic conditions in 1894. The crystalline solids, *o*-hydroxymethylphenol and *p*-hydroxymethylphenol were successfully isolated from the reaction, as shown in Figure 8. The importance of the Lederer-Manasse reaction was that it identified mild and well-controlled conditions for the condensation.

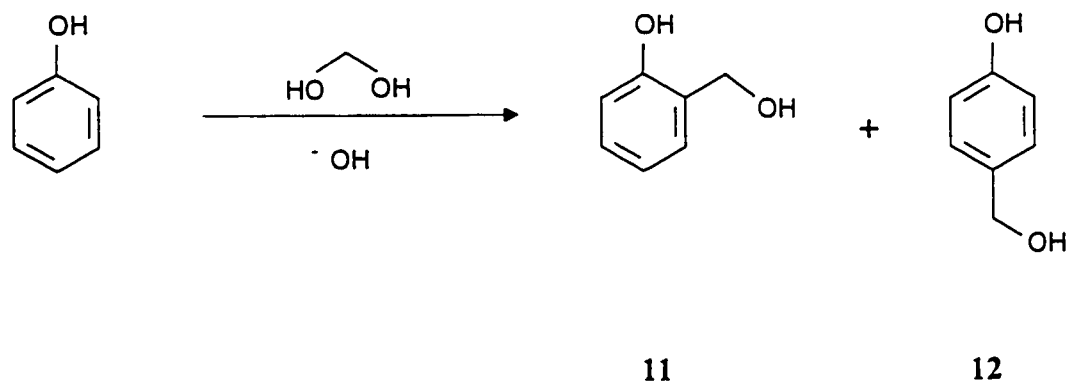
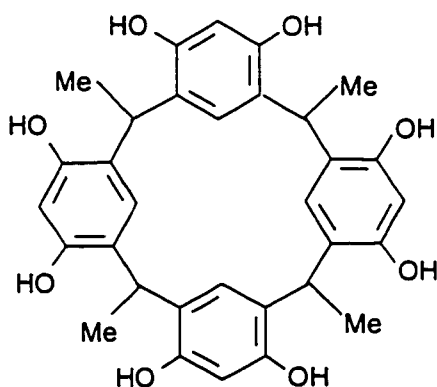


Figure 7. Lederer and Manasse's reaction.^{19,20}

As in the acid-catalyzed reaction, the aldehyde-phenol condensation yielded resin-like tar under strong basic conditions. In 1907 L. H. Baekland found that with small controlled amounts of base, the formaldehyde-phenol reaction would yield useful products. This process was named the Bakelite process, a process began the age of modern synthetic plastics.

In 1940, J. Neiderl and H. Vogel²² reinvestigated the Baeyer's experiments of the reaction between resorcinol and acetaldehyde, propionaldehyde and isovaleraldehyde, respectively under acidic conditions, and obtained high melting point materials. Based on the molecular weight data, it was suggested these solid products were best represented as cyclic tetramers (Figure 9). The eight hydroxyl groups in the Niederl's octols are extraannular. This class of compounds is now designated as calix[4]resorcinarenes or resorcin[4]arenes.



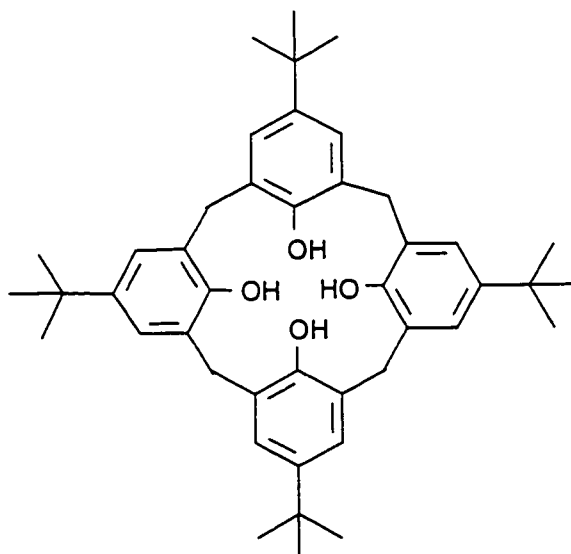
13

Figure 9. Structure of Neiderl's octols.

In 1942, A. Zinke and E. Ziegler²³ used *p*-alkyl substituted phenol for the base-induced formaldehyde-phenol process to make characterizable compounds. The product

12

of the reaction of *p-tert*-butylphenol with formaldehyde under mild basic conditions eventually lead Zinke and Ziegler²⁴ to propose a cyclic tetrameric structure with four intrannular hydroxyl groups. Figure 10 shows these kinds of compounds, which are now designated as calix[4]arenes. The cyclic structure was later confirmed by Zinke and co-workers.²⁵



8

Figure 10. Zinke and Ziegler's *p-tert*-butylphenol cyclic tetramer.

1.2.2 The Syntheses of Calixarenes and Calixresorcinarenes

The one-step, base-induced synthesis of phenol-derived calixarenes was originally formulated by Zinke²⁵, and then modified by Cornforth²⁶ and Gutshe.²⁷⁻²⁹ The amount of base used in the cyclooligomerization process affected the yields of different calix[n]arenes ($n > 4$). For example, optimum amount of cyclic tetramer was produced from 0.03 ~ 0.04 equivalents of the base, and with 0.30 or more equivalents of the base cyclic hexamer were the sole product. The formation of the cyclic tetramer is shown in Figure 11. From the study of the mechanism of formation of these oligomers, it has been postulated that the cyclic tetramer is the product of thermodynamic control, the cyclic hexamer the product of template control, and the cyclic octamer, the product of kinetic control.³⁰ Pure calixarenes have not been isolated from acid-catalyzed phenol-formaldehyde process, although there is some evidence that they are present in small amounts in the crude reaction mixture.³¹

A single compound was formed from the resorcinol-aldehyde reaction under acid-catalyzed conditions. Neiderl²² reported that the acid-catalyzed reactions of resorcinol with higher aldehydes than formaldehyde lead to cyclic tetramers in Figure 12. Högberg^{31,32} studied the reaction in detail and published a procedure that has been adapted to large-scale operation by Cram and co-workers³³ for the preparation of calix[4]resorcinarenes.

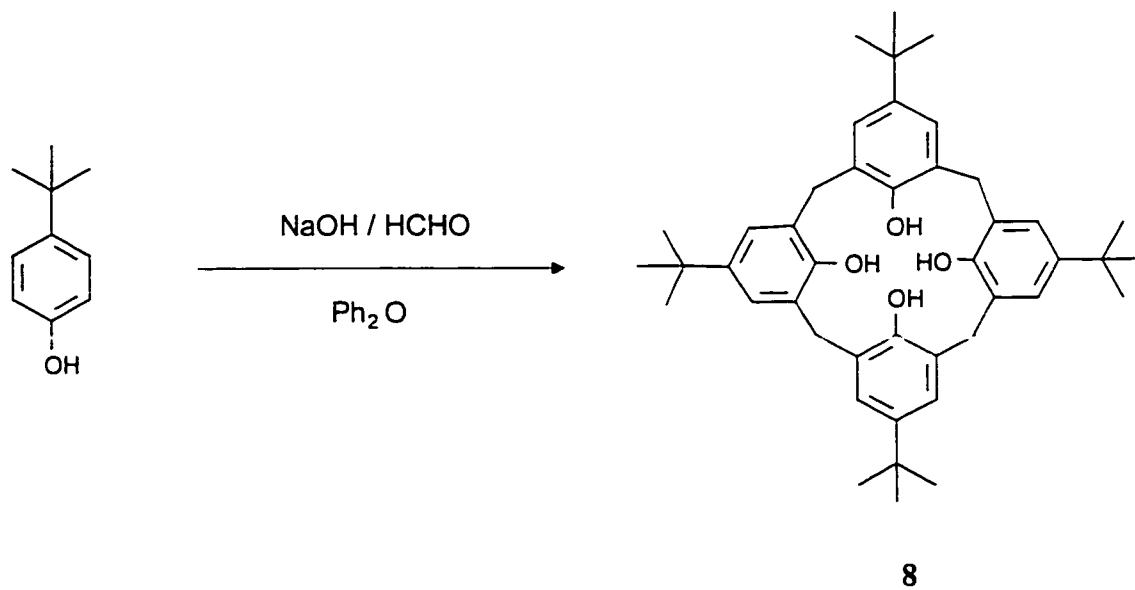


Figure 11. Zinke-Cornforth-Gutshe's procedure.

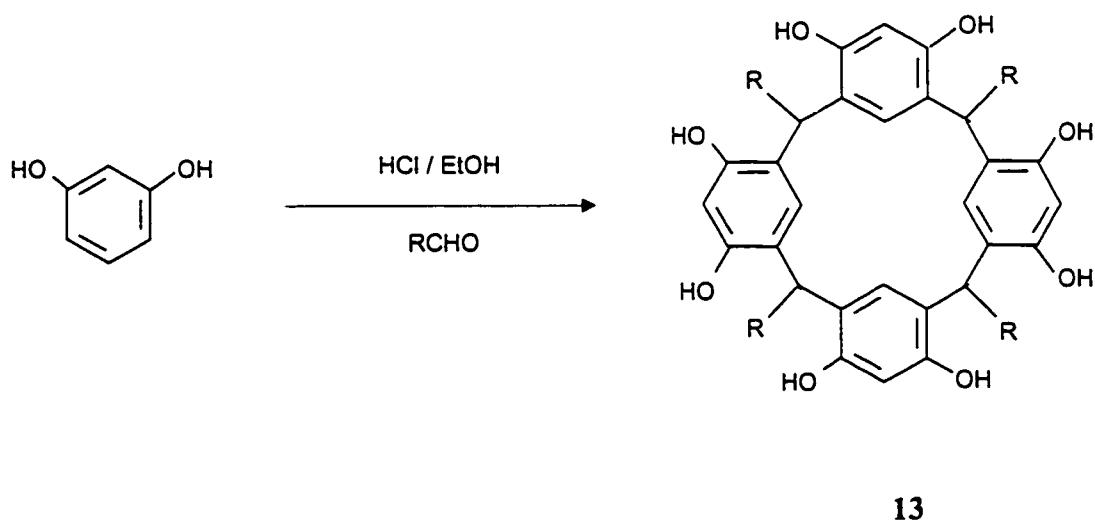


Figure 12. Neiderl-Högberg procedure.

1.2.3 Conformations of Calix[4]arene and Resorcin[4]arene

All of the calix[4]arenes were conformationally mobile in solution at room temperature.³⁴ In 1973, Cornforth and co-workers²⁶ postulated four potential conformations for a calix[4]arene as a result of the observation of two products obtained with identical molecular formulas and similar physical properties but different melting points. All four conformations were accessible by rotations of the aryl groups around the axis that passes through the *meta* carbon atoms bonded to the bridging methylene groups. The magnitude of the barrier of rotation of calix[4]arenes was reinvestigated with temperature-dependent ¹H NMR by Kämmerer and co-workers³⁵ and Gutsche and Bauer.^{36,37} The free energy of activation for *p-tert*-butylcalix[4]arene in chloroform solution was 15.7 kcal/mole and that for *p-pentyl*calix[4]arene was 14.5 kcal/mole. The four conformers of the calix[4]arenes have been designated as cone, partial cone, 1,2-alternate, and 1,3-alternate (Figure 13). The preferred conformer in solution is the cone, due to the cyclic hydrogen bonding of the four intraannular hydroxyl groups located at the lower-rim of the cone.³⁷

X-ray crystallography was first used by Ungaro and co-workers^{38,39} to ascertain one of these conformations. The X-ray structure of *p-tert*-butylcalix[4]arene was found to be the cone conformation as shown in Figure 14.

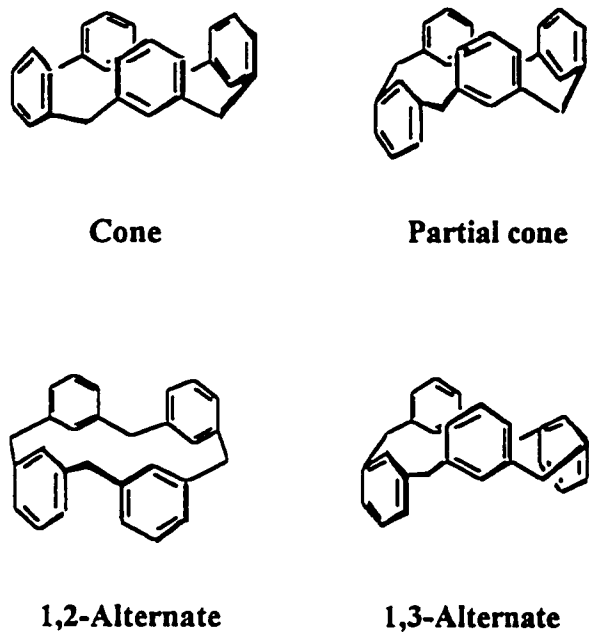


Figure 13. Calix[4]arene conformers.

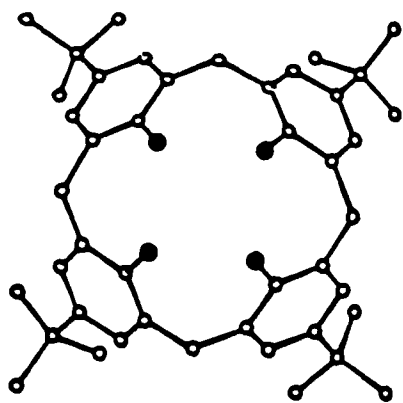


Figure 14. X-Ray crystallographic structure of *p*-*tert*-butylcalix[4]arene in the cone conformation.^{38,39}

In 1968, Högberg and Nilsson⁴⁰ first obtained a X-ray crystallographic structure of resorcin[4]arene from the Niederl resorcinol-benzaldehyde reaction to yield two isomeric compounds. One of these isomers of the *C-p*-bromophenylresorcin[4]arene octa-butyrate derivative was shown in Figure 15. A “boat-like” structure with arene rings which alternating nearly perpendicular was found, and such conformation did not correspond to the four conformers identified for the calix[4]arenes. The structure of another isomeric compound was not identified.

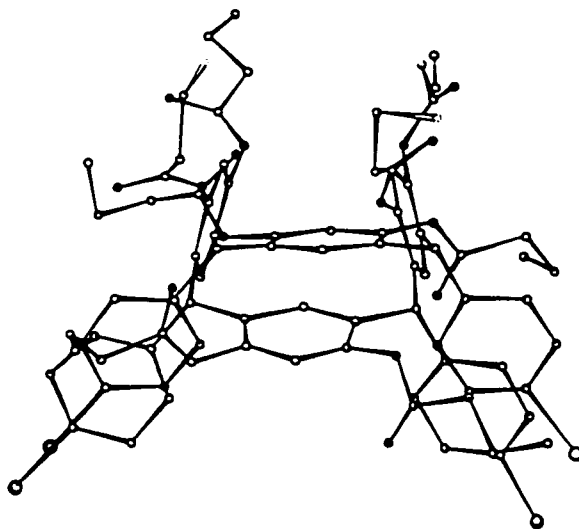


Figure 15. X-Ray crystallographic structure of Högberg-Nilsson's *C-p*-bromophenylresorcin[4]arene.⁴⁰

In Jurd's⁴¹ study of two isomers of *C-p*-bromophenylresorcin[4]arene octa-acetate derivative in 1976, a “chair-like” structure in which one arene ring was upward, another was downward and these two opposite arene rings were horizontal was identified. Another isomer was a similar to the conformation observed by Högberg (Figure 15).

The four conformations of resorcin[4]arene were postulated by Högberg⁴² based on the X-ray structures of the resorcin[4]arene derivatives. These conformers were designated as cone, flattened cone, 1,3-alternate, and flattened partial cone as illustrated in Figure 16. In 1989, the X-ray analysis showed *C*-butylcalix[4]resorcinarene and *C*-undecylcalixresorcin[4]arene as the cone conformation in the solid state⁴³ and in solution⁴⁴. As opposed to the lower-rim hydroxyl groups of the calix[4]arene, the resorcin[4]arene cone conformer has its eight hydroxyl groups located at the upper-rim of the arene rings.

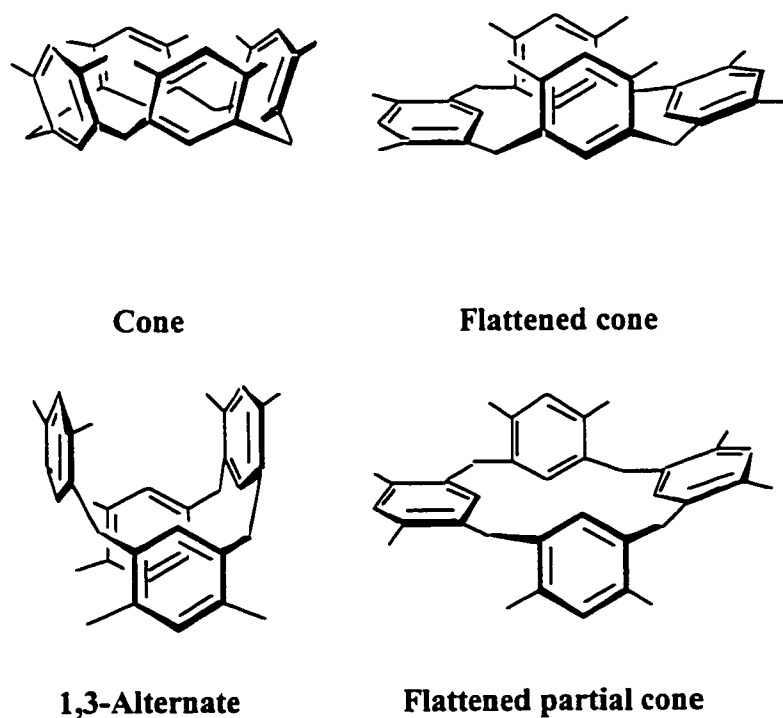


Figure 16. Calix[4]resorcinarene conformations.

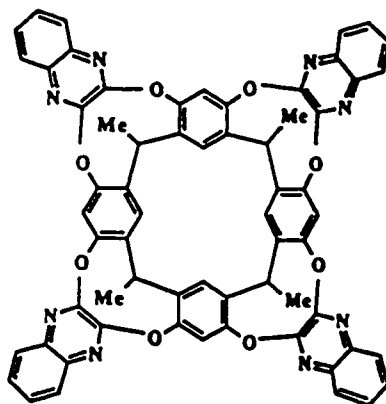
Recently, the resorcin[4]arene with no substituents on the methylene carbon atoms have also been found as the cone conformer by X-ray analysis.⁴⁵ The preferred cone conformation was a result of hydrogen bonds between the hydroxyl groups at the upper rim. The hydrogen bonding was much weaker than that in calix[4]arene based on the study of activated free energy by temperature-variable ¹H NMR technique. Previous work in our laboratory showed that the *C*-undecylcalix[4]resorcinarene octa-acetamide derivative in solution exhibited flattened cone conformation by variable temperature ¹H NMR.⁴⁶

1.2.4 Functionalized Calix[4]resorcinarenes

The eight hydroxyl groups of the calix[4]resorcinarene can be functionalized with electrophiles. Cram and co-workers have extensively investigated functionalized calix[4]resorcinarenes. The study was first carried out by the reaction between *C*-methylcalix[4]resorcinarene and bis-electrophiles such as ClCH₂Br, under basic conditions to link the adjacent hydroxyl groups and make the cavity more rigid. Such kinds of compounds shown in Figure 17 were named “cavitands”.⁴⁷ Subsequently, various functional groups like R = Br, CO₂H, CO₂Me, CH₂OH, CH₂Cl, and CH₂SH were introduced to the top carbon atoms of the arene rings. The cavitands with different linking groups of X = CH₂CH₂,³³ CH₂CH₂CH₂,³³ and Si(CH₃)₂⁴⁸ were also prepared. To make the cavitand more rigid and deeper, four equivalents of 2,3-dichloro-1,4-diazanaphalene were linked with the adjacent hydroxyl groups of calix[4]resorcinarene (14). Cram⁴⁸ has reported that the cavitands have unique features to complex solvent

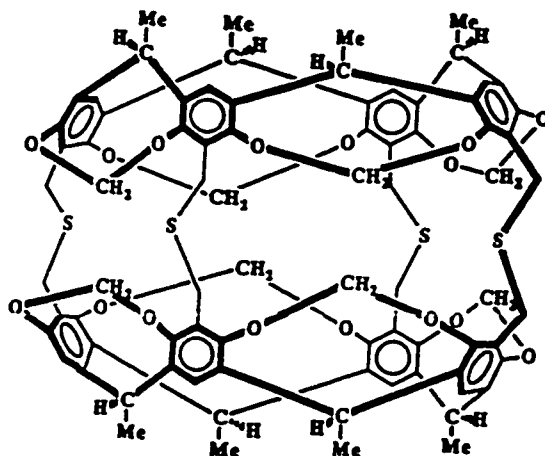
carbon disulfide, acetonitrile, chloroform, methylene chloride, benzene, toluene cyclohexane, and 1-propyne.

Probably, the most unusual of the host-guest complexes that have been synthesized are those involving carcerands.⁴⁹ The carcerands consist of a pair of cavitands joining upper rim to upper rim to create closed-surface, globe-shaped compounds with a vault large enough to incarcerate some of the small molecules present in the reaction milieu.⁵⁰ The linking groups were CH_2SCH_2 and OCH_2O groups as shown in Figure 18.



15

Figure 17. "Upper rim" bridged calix[4]resorcinarenes.⁴⁸



16

Figure 18. Structure of a carcerand.⁵⁰

Another interesting feature of carcerand chemistry is the development of the hemicarcerands. The hemicarcerands had only two or three bridges linking the two cavitands together, thus a portal was created to the interior of the molecule. The hemicarcerands exhibited an ability to introduce and release their guest molecules depending on temperature and to incarcerate larger molecules than carcerands.⁵¹ Cram used a hemicarcerand, as example, to securely incarcerate α -pyrone molecule. The sample was irradiated and the cyclobutadiene was formed inside the cavity of the hemicarcerand. Dimerization or other reactions of cyclobutadiene were prevented by the protection of the molecular shell, and the encapsulated cyclobutadiene was spectroscopically identified.⁵²

1.2.5 Calix[4]resorcinarenes as Host Molecules

Aoyama and co-workers⁴⁴ in 1989 reported the calix[4]resorcinarenes as lipophilic polar hosts to bind nonionic polar and water-soluble compounds in apolar media. The study showed that *C*-undecylcalix[4]resorcinarenes are able to complex water,⁵³ glycerol,⁵³ diols,^{44,54} sugars,^{44,55} dicarboxylic acids,⁵⁶ steroids,⁵⁷ and chiral alcohols.⁵⁸ The binding in these complexes was a result of hydrogen bonding between the oxygen atoms and the hydrogens (Figure 19). The adjacent binding sites locate on the proximate OH groups of the calix[4]resorcinarene.

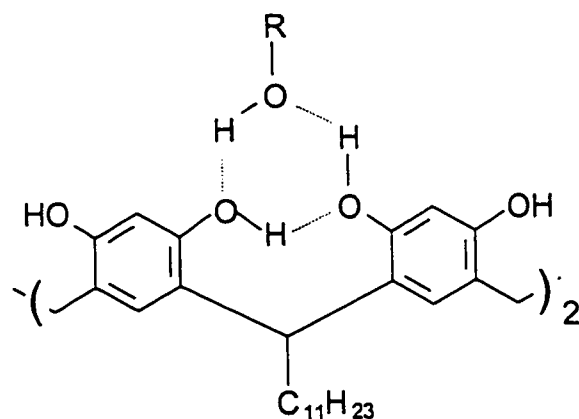


Figure 19. Hydrogen bonding at proximate OH groups of the calix[4]resorcinarene.⁴⁴

Schneider^{59,60} studied the *C*-methylcalix[4]resorcinarene as host molecule toward ammonium ions in basic aqueous solution. Trimethyl *n*-propyl- and tetramethyl-ammonium salts were complexed to a greater degree than tetraethyl-, tetrapropyl-, tetrabutyl-, and triethyl benzyl-ammonium salts. Based on CPK model in the complexes

with N^+ -Me guest molecules, the N^+ atoms locating just above the upper-rim effectively bound with anionic phenyl parts of the macrocycle by electrostatic attraction.⁵⁹ The stronger complexation with R_3N^+Me was demonstrated in larger complexation-induced changes in the 1H NMR chemical shifts, as shown in Table 2.

Table 2. Complexation-Induced 1H NMR Shifts (CIS).

guest molecule	proton	CIS (ppm)
N^+Me_4	CH_3	1.84
N^+Et_4	CH_3CH_2	1.19, 1.18
N^+n-Bu_4	all H	<0.01
N^+Me_3, n -Propyl	$CH_3, CH_2CH_2CH_3$	2.02, 1.20, 0.5, 0.1
N^+Et_3, CH_2 -Ar	CH_3CH_2, CH_2 -Ar	1.41, 1.21, 0.79
N^+n -Propyl ₄	$CH_3CH_2CH_2$	0.42, 0.42, 0.42

C-methylcalix[4]resorcinarene was also studied for the binding of alkali metal by Koide.⁶¹ Cesium ions were selectively bound from mixtures of Li^+, Na^+, K^+, Rb^+ , and Cs^+ ions.

Previous work in our laboratory⁴⁶ showed that the *C*-undecylcalix[4]resorcinarene functionalized with octa-amide has strong binding toward silver ion (Ag^+) compared to *t*- $BuNH_3^+, NH_4^+, Na^+, K^+, Rb^+$, and Cs^+ ions. The 1H NMR chemical shift in the aromatic protons proved such complexation. In the comparison with unbound 1H NMR spectrum,

protons proved such complexation. In the comparison with unbound ^1H NMR spectrum, the lower-rim aromatic protons in the bound spectrum were shifted upfield, and the upper-rim protons were downfield shift.⁴⁶ It was suggested that the binding of the metal cation is in a 1:1 complex with the host as shown in Figure 20.

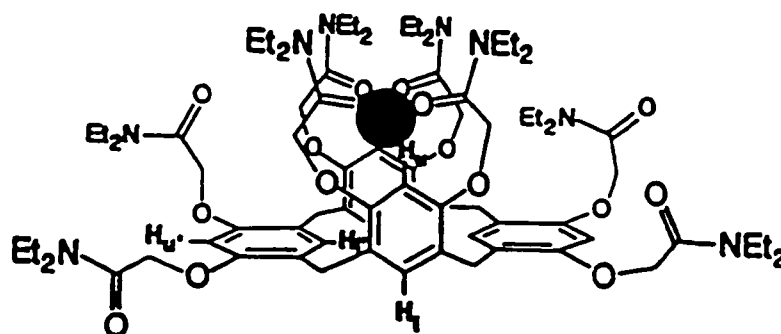


Figure 20. Bound silver ion within the cavity.⁴⁶

The studies of resorcinarenes as host molecules discussed so far were all carried out in solution, the techniques for the preparation of well-ordered systems has recently been expanded to study on the resorcinarenes binding metal in well-organized Langmuir-Blodgett films. The luminescence characteristics of terbium ion (Tb^{3+}) incorporated into undecylcalix[4]resorcinarene octa-amide derivative in the LB films was observed.⁶²

1.3. Langmuir-Blodgett Films

Monomolecular assemblies on substrates, now termed Langmuir-Blodgett (LB) films, have been studied for over half a century. In the late 1917, Irving Langmuir⁶³ focused on the study of monolayers on water surface, and developed the surface film balance to measure the spreading pressures of thin films. Langmuir confirmed that his films had the thickness of a single molecular layer and also concluded that the molecules were oriented at the water surface, with the polar functional group immersed in the water and the long nonpolar chain directed almost vertically from the surface.⁶⁴ Due to his efforts on Langmuir films Langmuir was awarded the Nobel Prize in 1930.⁶⁴ Katharine Blodgett⁶⁵, under Langmuir's guidance, successfully transferred fatty acid monolayers and multilayers from water surfaces to solid supports such as glass slides. Therefore, monolayer assemblies on substrates are now referred to as Langmuir-Blodgett (LB) films as distinct from Langmuir films, a term reserved for a floating monolayer.⁶⁴

1.3.1. Formations of Langmuir Films and Langmuir-Blodgett Films

1.3.1.1 Surface Pressure/Area Isotherms

The surface pressure/area isotherm usually abbreviated as " π - A isotherm" or "isotherm" is a plot of surface pressure as a function of the area on water surface at constant temperature. The monolayer properties of a material such as molecular sizes and intermolecular forces can be obtained from such plot.⁶⁶

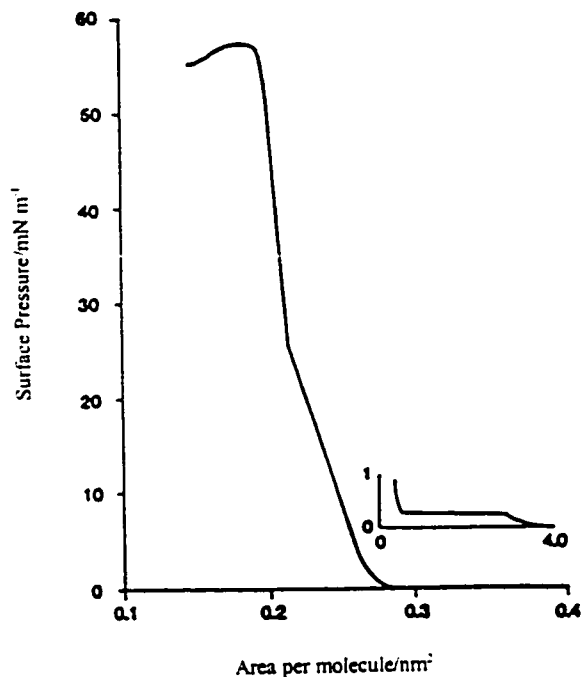


Figure 21. Surface pressure/area isotherm of stearic acid on an acidified aqueous subphase.⁶⁶

Figure 21 is a typical π - A isotherm. Different regions of Langmuir films could be illustrated clearly from analysis of the isotherm.⁶⁶ The surface pressure of zero or very small illustrated the weakness of interaction between water and the tail group. This indicated the hydrophobic chains originally distributed near the water surface (Figure 22a). The second region was of a phase change from liquid-expanded to liquid-condensed phase transition when the slope increased rapidly. This indicated the tail groups were being lifted away (Figure 22b). Then, there was a steeply sloping linear region that represents liquid-condensed phase,⁶⁷ an ordered solid-like arrangement of the two-dimensional array of the molecules on aqueous surface (Figure 22c). If this linear portion is extrapolated to

zero surface pressure, the intercept, named “limiting area” gives the area per stearic acid molecule. The limiting area value is close to the stearic acid molecular area in single crystals, thus confirming the compact film as a two-dimensional solid.⁶⁶

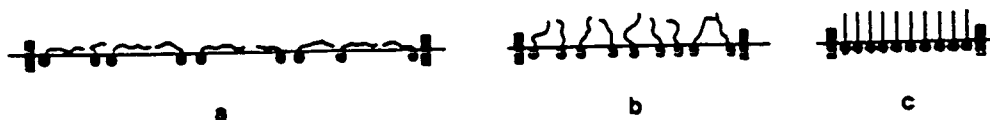


Figure 22. Monolayer of stearic acid on a water surface: (a) expanded, (b) partly compressed, (c) close packed.⁶⁶

In the π - A isotherm (Figure 21), the Langmuir film collapses when the linear relationship between surface pressure and molecule area deviates the linear region when surface pressure increases. It is believed that a well-ordered Langmuir film is changed to disordered multilayers, in which the molecular layers are riding on top of each other, as schematically shown in Figure 23.

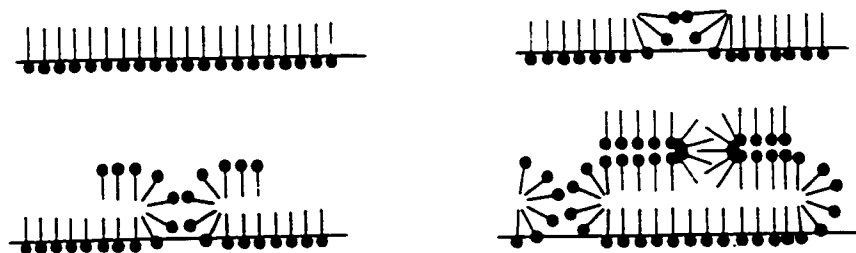


Figure 23. Collapse of Langmuir film.⁶⁶

1.3.1.2 Langmuir-Blodgett Deposition

Langmuir film of a material can be transferred from subphase to substrate using the Langmuir-Blodgett technique.⁶⁶ The Langmuir film is transferred to the substrate by mechanically dipping and withdrawing the substrate into subphase such as water. In order to maintain constant conditions during this process the surface pressure is kept constant mechanically, usually using the films in the liquid-condensed phase.⁶⁸ If the slide used has a hydrophilic surface, deposition follows the sequence of events schematically shown in Figure 24. The water wets the slide's surface and the meniscus turns up (Figure 24a). As the slide is withdrawn the meniscus is wiped over the slide's surface and the leaves behind a monolayer in which the hydrophilic groups are turned toward the hydrophilic surface of the slide (Figure 24b). The rate at which a slide can be withdrawn from the water is typically about 1 mm/s.⁶⁸

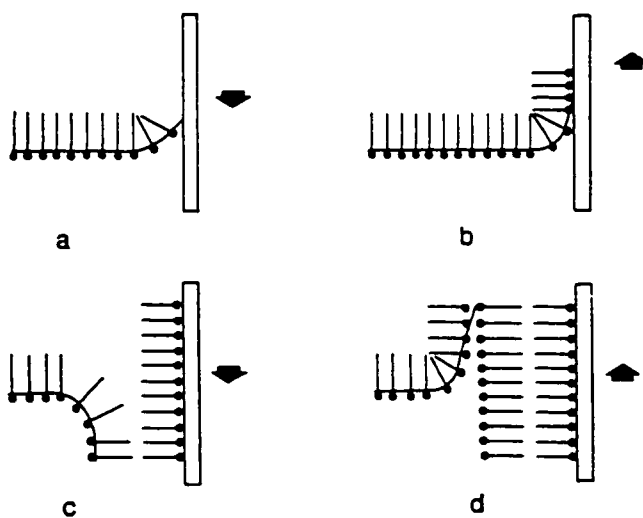


Figure 24. Deposition of multilayers by the LB technique: (a) first immersion, (b) first withdrawal, (c) second immersion, (d) second withdrawal.⁶⁸

The second dip into the subphase (Figure 24c) differs from the first in that the slide is now hydrophobic, the meniscus turns down and a second monolayer is deposited with its tail groups in contact with the exposed tail groups on the slide. The second withdrawing from the subphase exactly resembles the first. This type of deposition, known as Y type, is shown in Figure 25. It is also possible to have deposition occur only when the substrate enters the subphase (X type) or leaves it (Z type), depending upon the nature of the monolayer, substrate, subphase, and the surface pressure.

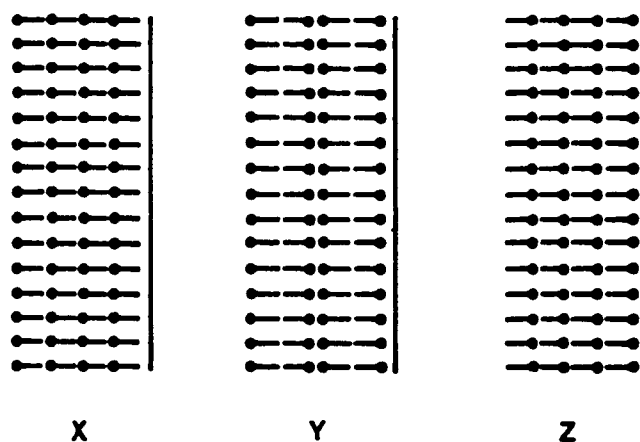


Figure 25. Structures of X, Y, and Z type depositions.⁶⁸

1.3.2. Types of Molecules to Form Langmuir Films and Langmuir-Blodgett Films

1.3.2.1 Fatty Acids and Derivatives

When the subphase pH < 8.2, fatty acids containing more than 13 carbon atoms can be spread to form a monolayer, but the stability varies greatly with chain length.⁶⁹ For example, myristic acid (n = 13) showed a loss of 0.1%/min from the surface area of a

monolayer at 20°C and 10mN/m. It is caused by material dissolving into the subphase. In contrast, stearic acid ($n = 17$) would loss less than 0.001%/min under similar conditions.⁷⁰

The modified alkyl (hydrophobic) tail groups of fatty acids can affect the monolayer behavior. For example, the oleic oxide π -A isotherm (Figure 26) did not show a clear liquid-condensed phase and had a larger area per molecule compared to oleic acid.⁷¹ The difference in the π -A isotherm was interpreted that the hydrophilic character of the epoxide group causing the molecule to arch over to also contact aqueous subsphase and occupy a relatively large surface area. When the surface pressure is increased sufficiently, the second point of contact is detached and the area per molecule thereby reduced. It was not possible to build up multilayers of this molecule using the LB technique. The longer chain ($n = 21$) terminal epoxide gives a more conventional isotherm and can readily be built up as multilayers.⁷²

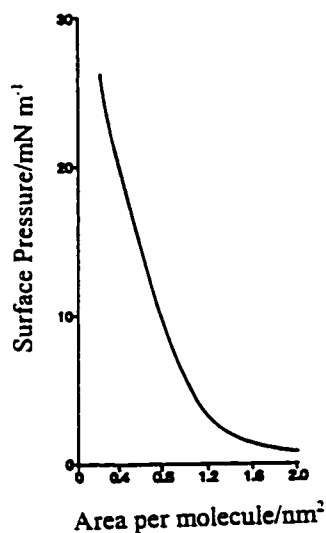


Figure 26. Surface pressure/area isotherm of oleic epoxide (19°C, pH = 3.5).⁷²

1.3.2.2 Aromatic Hydrocarbons Derivatives

The derivatives of anthracene have been more extensively investigated than any other groups of materials except the fatty acid derivatives.^{73,74} The isotherms of the anthracene derivatives with hydrophilic group and long hydrophobic chains indicated that the stable films were obtained from the long hydrophobic chains.

Böhmer and co-workers⁷⁵ in 1982 first successfully made stable Langmuir films and LB films of *p*-octadecylcalix[4]arene from a basic subphase. In the last 10 years, Shinkai's group⁷⁶⁻⁷⁹ has focused on metal ions selectively complexed in calixarenes in Langmuir films. As example, Figure 27 presents the π -*A* isotherms of *p*-*tert*-butylcalix[*n*]arene ester derivatives.

The limiting areas (molecule size) of calixarene esters (Figure 27a) were in accord with the areas of the large sides (the upper rim) of the cone-type calixarene cavity, which were estimated from the X-ray data by Ungaro⁸⁰ and McKervey⁸¹ and by Corey-Pauling-Koltun (CPK) models. The results also showed the calixarene ester derivatives selectively binding metal ions in the subphase (Figure 27b). The observation was in agreement with the ion recognition for the calixarenes in solution.⁸² It was believed that the monolayers selectively complex the metal ions through the ionophilic ester groups (Figure 28). In another laboratory the *p*-*tert*-butylcalix[6]arene was found to exhibit a high selectivity to Cs⁺ at the water-air interface compared to Na⁺ and K⁺.⁸³ The monolayer expansion induced by the metal complexation was unclear. The expansion may result of the conformational change, or by the electrostatic repulsion among bound

Our laboratory has studied the monolayer properties of *C*-undecylcalix[4]resorcinarene⁸⁴ and its ester derivative (-CH₂CO₂Me, CALES) and amide derivative (-CH₂CONEt₂, CALAM).⁸⁵ Multilayers of CALES were obtained, but it was not possible to make multilayers of CALAM from an aqueous subphase or from a subphase containing metal cations. The UV-visible spectra proved that both CALES and CALAM exist in the conformation of the flattened cone.⁸⁵

In addition, there have been many publications about the monolayers of calix[4]resorcinarenes deposited on substrate by self-assembly technique that is different from the LB deposition. As one of most active groups in this field, Reinhoudt and co-workers have many papers on the cavitands derived from resorcin[4]arene with four dialkylsulfides as tailgroups^{86,87} and carceplexes⁸⁸ forming stable monolayers on gold surfaces.

1.4 Objective

Previous work has shown the failure of tetra-tailed resorcinarene amide derivative such as CALAM to form multilayer LB films.^{62,85} The modification of the tetra tailed to the octa tailed will theoretically increase cross sectional area of the alkyl tail chains to be close to the amide head group area. The anticipated effect of this change is shown schematically in Figure 29. A minimum estimate of the area of four methylene chain is 0.96 nm², which is based on the limiting area of arachidic acid $A = 0.24 \text{ nm}^2$. This is smaller than the areas of hydroxyl head group of *C*-undecylresorcin[4]arene ($A = 1.4$

nm²) and areas of ester head groups ($A = 1.6 \text{ nm}^2$) and amide head groups ($A = 2.7 \text{ nm}^2$).

Eight methylene chains in the tail section will increase the minimum area to 1.92 nm^2 .

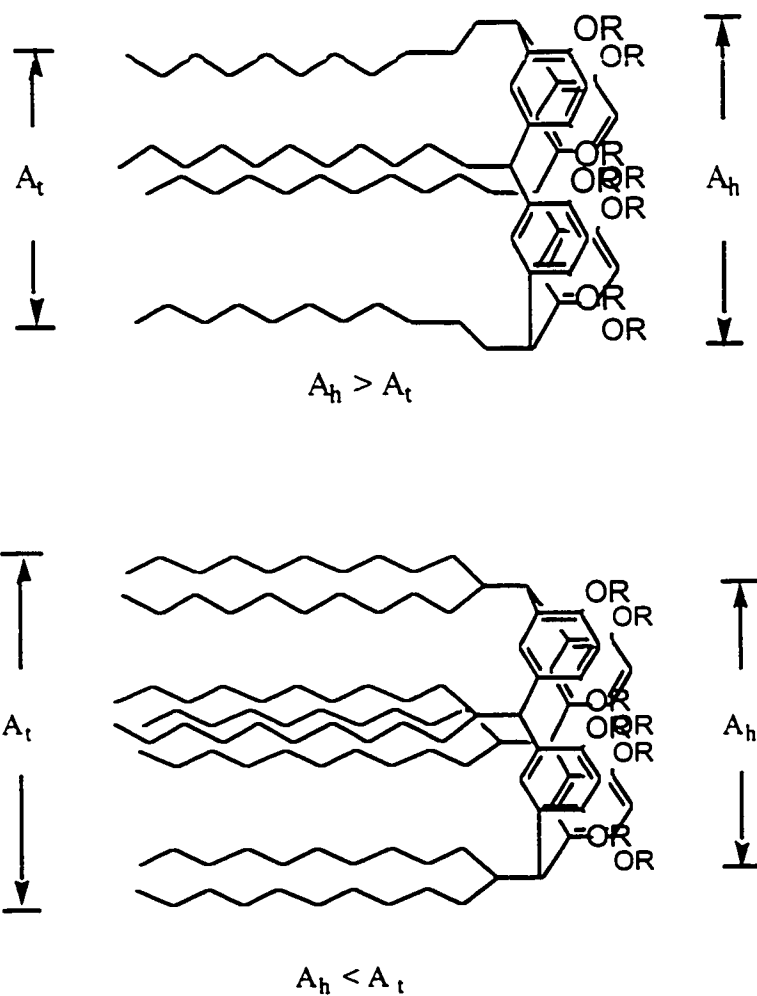


Figure 29. Theoretical head and tail sizes of four-tailed resocin[4]arene and eight-tailed resorcin[4]arene.

This structural modification would improve the hydrophobic-hydrophobic (tail-to-tail) interaction or the hydrophilic-hydrophobic (head-to-tail) interaction between the monolayers to form multilayer LB films of the amide derivative. Also, the increase in the tail group area may allow the flattened cone conformation for functionalized resorcin[4]arenes which was observed in solution to manifest itself in the LB films.

There has been no report of the preparation of octa-tailed resorcin[4]arenes and the monolayers and LB films of these materials. Some interesting behavior of the LB films of the octa-tailed resorcinarenes, such as multilayer LB films or flattened cone conformation in the LB films could be observed. Therefore, our project was first to synthesize the octa-tailed calix[4]resorcinarenes and latter to investigate the behavior of their monolayers and LB films. The project included: a) the syntheses of calix[4]resorcinarenes with long and short octa-tail groups and tetra-tail groups and their derivatives of ester and amide; b) study of conformations of these octa-tail compounds in solution; c) fabrication of monolayers and LB films of these octa-tailed and tetra-tailed compounds from aqueous subphase or from the subphase containing metal cations; d) characterization of the octa-tailed compounds on the monolayers and the LB films by comparison with the tetra-tailed compounds.

2. RESULTS AND DISCUSSION

2.1. Synthesis

2.1.1 α,α -dihexyl acetaldehyde

There have been reported various tail groups incorporated on the methylene positions of calix[4]resorcinarene by changing the aldehydes used in the preparation of resorcinarenes.^{32,44,89,90} The starting materials of aldehyde with a long branched group $R = \text{CH}[(\text{CH}_2)_5\text{CH}_3]_2$ at α position of the carbonyl was synthesized by following Kluge's procedure,⁹¹ as shown in Figure 30.

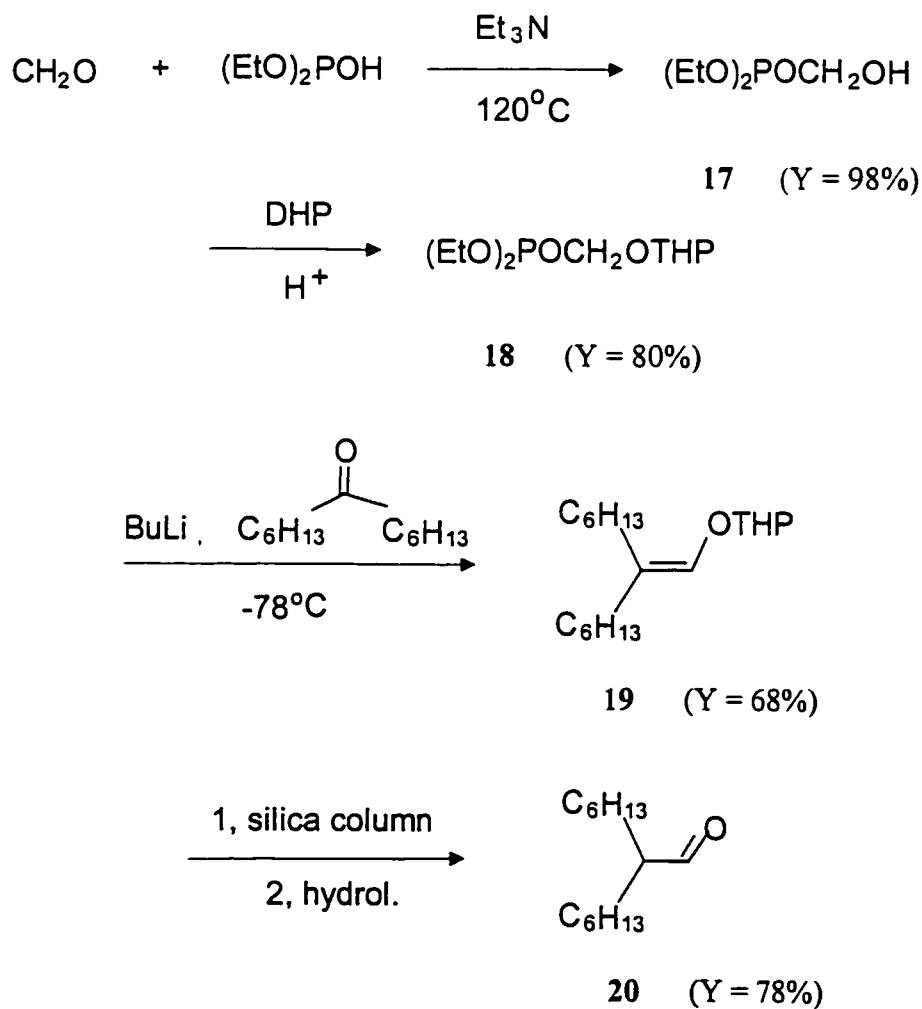


Figure 30. Synthesis of α,α -dihexyl acetaldehyde.

Modifications to the Kluge's procedure were required in our synthetic process. Based on ^1H NMR analysis the pure phosphonate **17** was obtained by evaporation at 60°C under vacuum for 2 hrs with substitution of Kugelrohr distillation described in the literature. The excess triethylamine as a catalyst was evaporated out under vacuum after the reaction. This modification was to improve the yield and simplify the purification. The complete preparation of phosphonate **18** at least took 4 hrs based on TLC analysis using 50% ethyl acetate/petroleum ether. A high yield of the intermediate enol ether **19** could also be obtained at -78°C instead of -100°C . Our experimental results showed that it is impossible to completely isolate the intermediate from impurities by filtration using 10% ethyl acetate/hexane solvent as described in the literature. The purification procedure was modified by using column chromatography with 2% ethyl acetate/petroleum ether. The aldehyde **20** was obtained by 12-hr hydrolysis of the enol ether **19** in reflux under acidic conditions rather than 4-hr hydrolysis at room temperature due to high hydrophobicity of **19** containing long branched chains. The pure **20** was obtained as colorless oil after column chromatography, and it was characterized by ^1H and ^{13}C NMR, IR, and MS techniques, which were identical to literature data. The ^1H and ^{13}C NMR spectra in Figures 31 and 32 illustrated purity (>95%) of **20** was adequate for subsequent steps.

The doublet signal at 9.56 ppm in Figure 31 was assigned to the aldehydic proton, which is split by adjacent methine proton. The sextet signal at 2.23 ppm was assigned to the methine proton that is split by adjacent five protons (four methylene protons at the

hexyl chains and one aldehydic proton). The remaining peaks represented the hexyl chains.

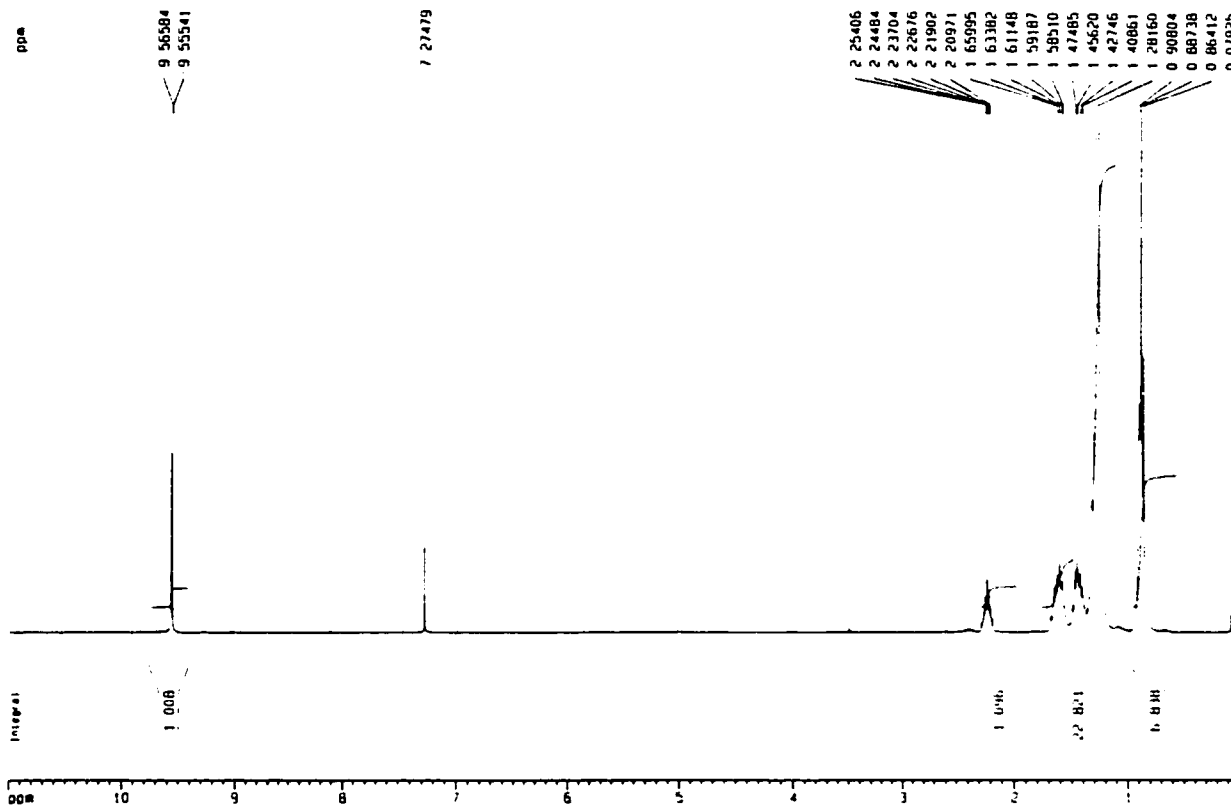


Figure 31. ^1H NMR spectrum of 20.

In the ^{13}C NMR spectrum (Figure 32), a signal at 205.96 ppm was assigned to carbon atom in the carbonyl group. The methine carbon atom was represented by a signal at 52.25 ppm. The remaining six signals were assigned to six carbon atoms of the branched hexyl chains.

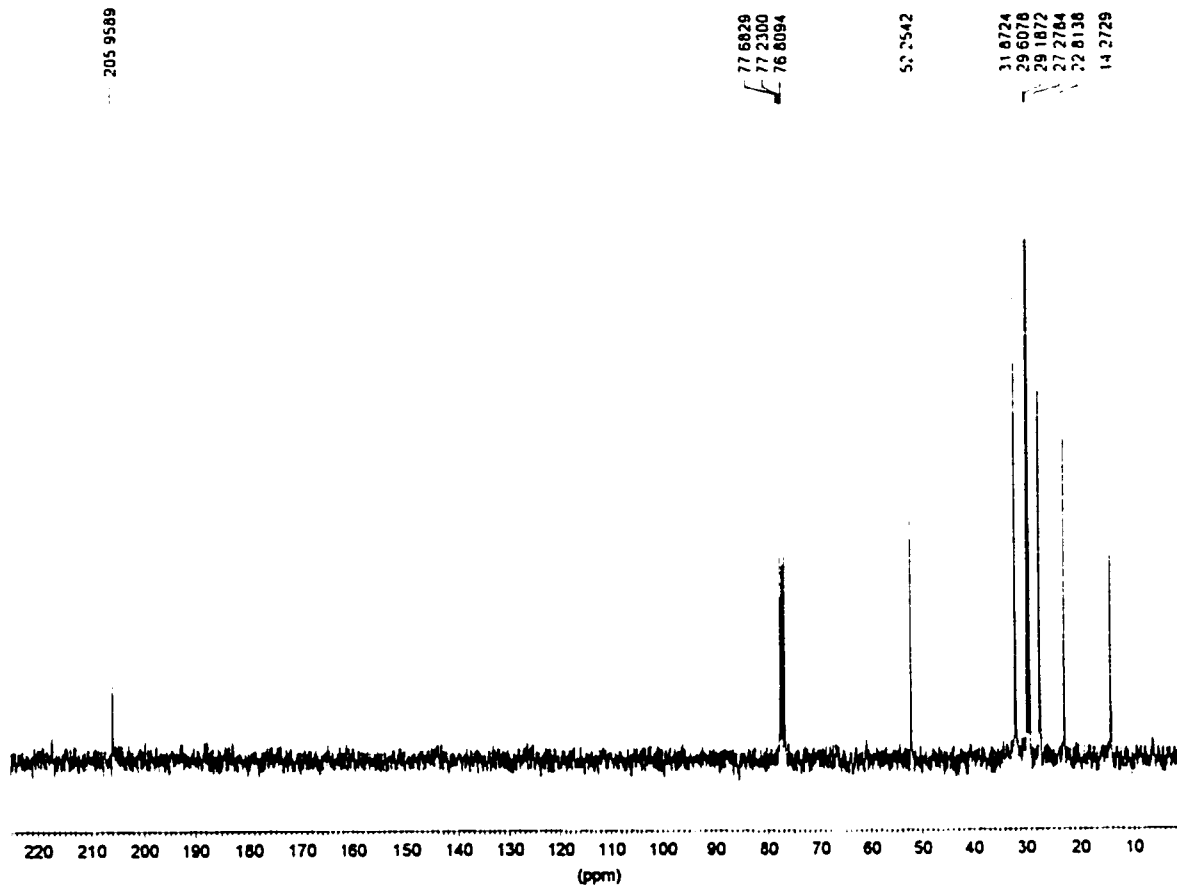


Figure 32. ^{13}C NMR spectrum of 20.

In addition, the 20 was found to be partly oxidized to the carboxylic acid after it was stored in refrigerator ($\sim 4^\circ\text{C}$) for three months. In order to avoid the oxidation, the crude aldehyde obtained after the hydrolysis should be neutralized, and stored under nitrogen at -4°C . The mass spectra of the oxidized aldehyde and the pure aldehyde are shown in Figure 33. Molecular ion of 20 was presented by a signal at $m/e = 212$ (M^+), a signal at $m/e = 182$ was assigned to a fragment of $[\text{CH}_3(\text{CH}_2)_5]_2\text{CH}^+ - \text{H}$, a signal at $m/e = 229$ was assigned to molecular ion of α,α -dihexyl acetic acid ($\text{M} + \text{H}$), and a signal at $m/e = 458$ was assigned to its dimer. Two molecules of the acid were combined through hydrogen binding at the carboxyl groups.⁹²

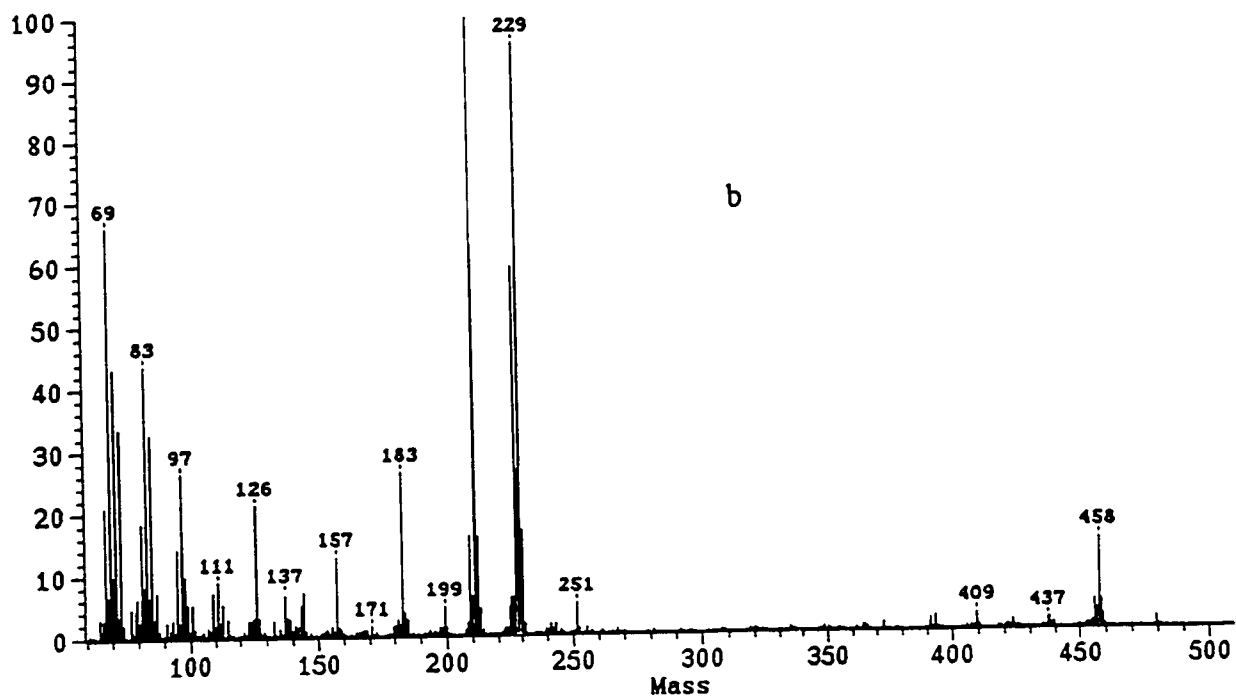
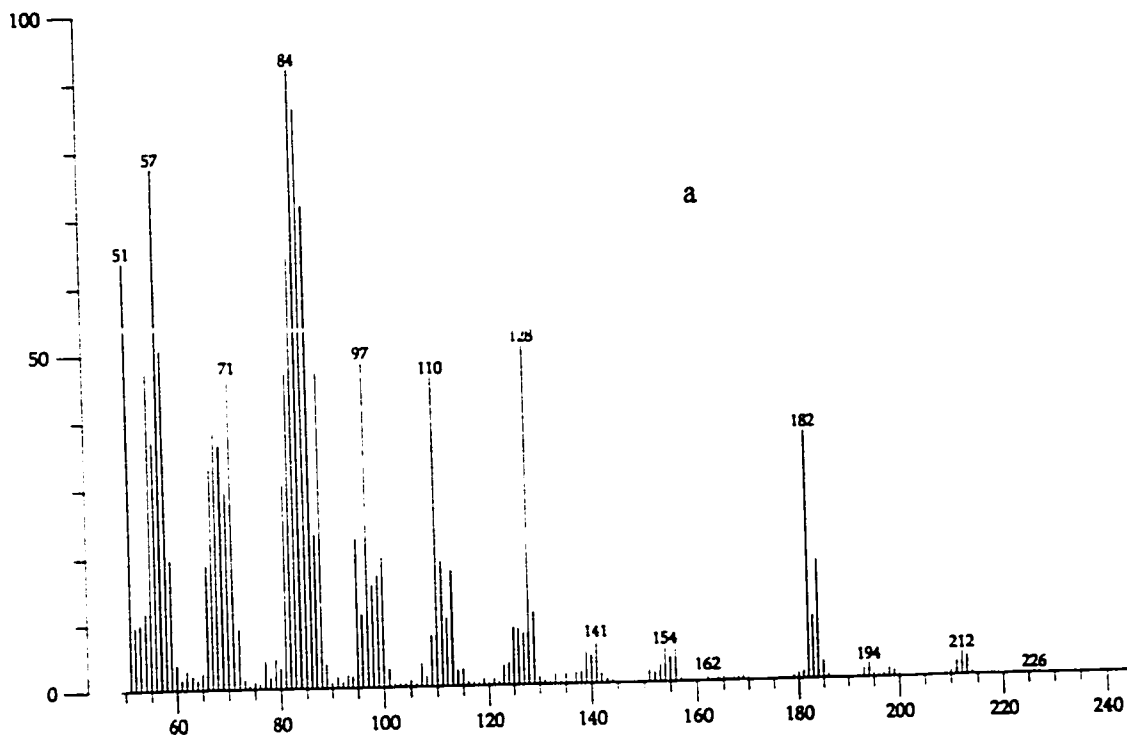


Figure 33. MS spectra of (a) pure and (b) oxidized 20.

2.1.2 Octa-Tailed Calix[4]resorcinarenes

Various tetra-tailed calix[4]resorcinarenes have been prepared in our laboratory. The octa-tailed calix[4]resorcinarene with a short branched group $R = \text{CH}(\text{CH}_3)_2$ was prepared in order to ensure that the cyclooligomerization would proceed.

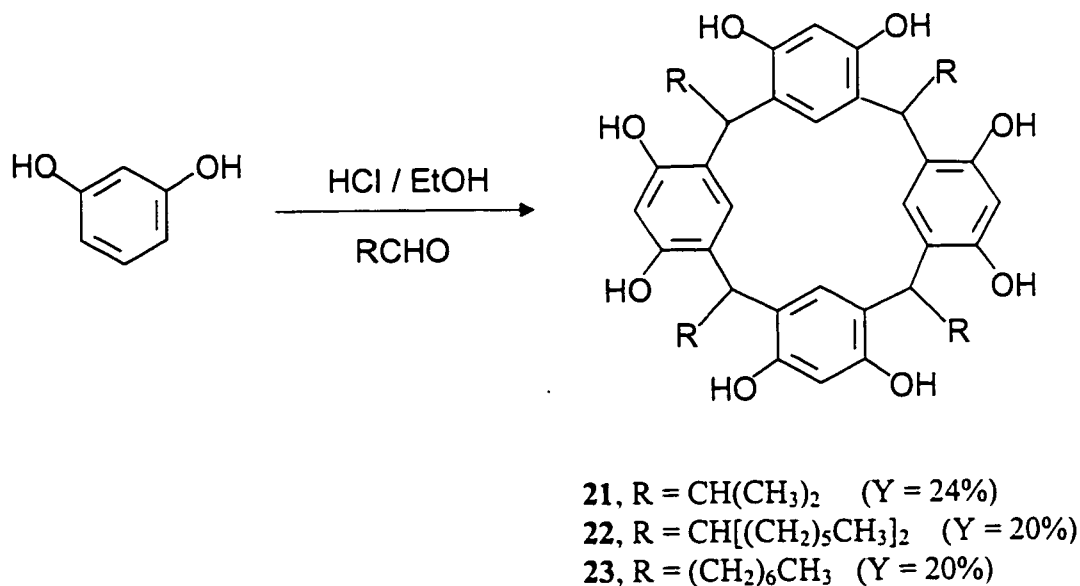


Figure 34. Synthesis of calix[4]resorcinarenes.

Figure 34 is preparation of the octa-tailed resorcinarenes, **21** and **22** by the cyclooligomerization of resorcinol with isobutyraldehyde and **20** respectively under acidic conditions, following the procedure of Aoyoma.⁴⁴ Compound **21** was prepared at 60 ~ 70°C for 24 hrs and by recrystallization from a mixture of ethyl acetate/cyclohexane (1:10). In order to complete the reaction, preparation of **22** had to take 72 hrs at the same temperature. Purification of **22** was performed by column chromatography on silica gel with 50% ethyl acetate/petroleum ether. It was not possible to obtain pure **22** by recrystallization. A quite low yield of the resorcinarenes was mainly as a result of the

column chromatography process. Generally, the yield of the crude products of **21** - **23** was around 75% obtained in our experiments.

Table 3. The data of ^1H NMR of **21** and **22**.

functional group	21	22
	(ppm)	
ArH lower rim	7.10	7.16
ArH upper rim	6.10	6.04
Ar-CH-Ar	3.86	3.96
Ar-CH-CH[(CH ₂) ₅ CH ₃] ₂	-	3.52
Ar-CH-CH(CH ₃) ₂	2.80	-
Ar-CH-CH[CH ₂ (CH ₂) ₄ CH ₃] ₂	-	2.32
Ar-CH-CH[CH ₂ (CH ₂) ₄ CH ₃] ₂	-	1.16
Ar-CH-CH(CH ₃) ₂	0.85	-
Ar-CH-CH[(CH ₂) ₅ CH ₃] ₂	-	0.78

The two octa-tailed resorcinarenes, **21** and **22** were characterized by ^1H and ^{13}C NMR, IR, MS analyses, and melting point. The ^1H NMR data are listed in Table 3. The eight aromatic protons were represented by two signals in the region of 6.0 to 7.2 ppm in which the four lower-rim protons (meta to the hydroxy groups) were shifted further downfield than the four upper-rim protons (ortho to the hydroxy groups). This is correlated with higher electron densities at the ortho protons shielded at upper field than at the meta protons. The four methine protons connected with the tail alkyl chains were

represented by one signal at around 3.9 ppm. The above observation indicates a four-fold symmetry (C_{4v}) of **21** and **22** on the NMR time scale. This illustrates **21** and **22** as a cone conformer in solution. The cone conformer is preferred in solution due to the cyclic array of hydrogen bonding of the eight extraannular hydroxyl groups located at the upper rim of the resorcinarene.⁴⁵

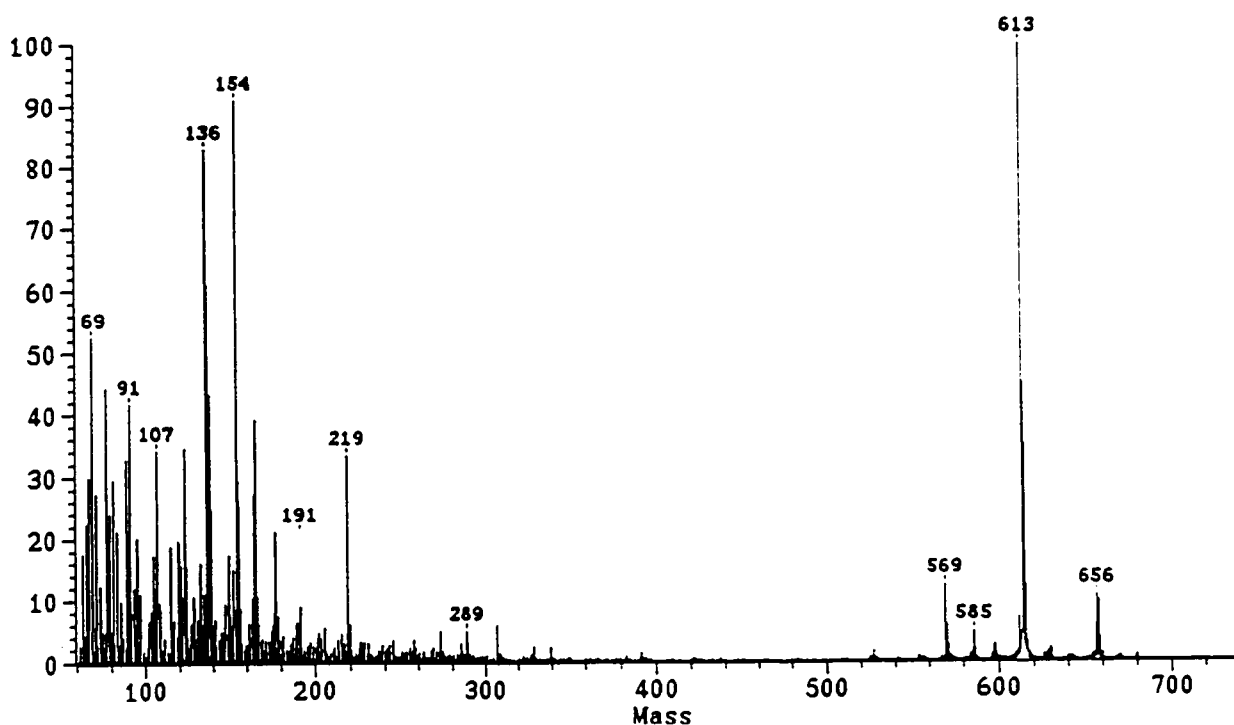


Figure 35. MS spectrum of **21**.

The mass spectrum in Figure 35 presents a signal at $m/e = 656$ (M^+) that was assigned to molecular ion of **21** and a fragment signal at $m/e = 613$ ($M - R$). The $R =$ isopropyl group is the tail alkyl chains of **21**. Molecular ion of **22** was observed at $m/e =$

1216 (M^+) in Figure 36. A fragment of 22 losing one tail alkyl chain, $R = CH[(CH_2)_5CH_3]_2$ was assigned at $M - R = 1033$. The MS data illustrate a relatively stable structure of the calix[4]resorcinenes losing one tail alkyl chain. This can be explained a tropyllium ion formation.

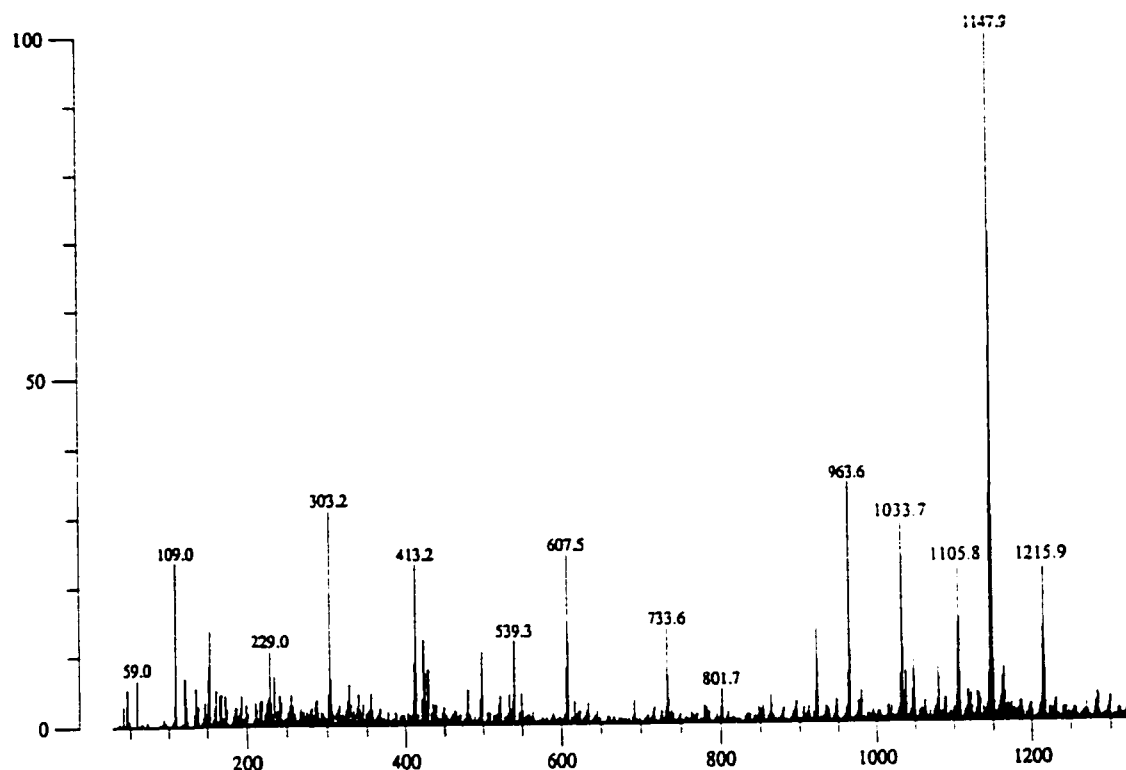


Figure 36. MS spectrum of 22.

The melting points of 21 and 22 were above 300°C and 134-136°C, respectively.

2.1.3 Octa-Functionalized Calix[4]resorcinarenes

Previous work in our laboratory has shown the physical characteristics of binding metal and ammonium ions. A strong selectivity for *C*-undecylcalix[4]resorcinarene functionalized with diethyl amide, compared to other functional groups such as methyl

ester and *tert*-butyl ester.⁴⁶ Therefore, compound **22** functionalized with *N,N*-diethyl acetamide and methyl acetate were prepared and the characteristics in solution and Langmuir-Blodgett films were investigated.

2-Bromo-acetyl bromide was purchased from the Aldrich Chemical Company. 2-Bromo-*N,N*-diethylacetamide was prepared by following a known procedure.^{93,94} The reaction of excess diethylamine (2:1 molar ratio) with the 2-bromo-acetyl bromide was carried out at -10°C to give 2-bromo-*N,N*-diethylacetamide (**24**) in a yield of 81% (Figure 37). The ¹H and ¹³C NMR spectra matched those reported in literature.⁹⁴ The amide, **24** was covered with parafilm and stored in refrigerator prior to use.

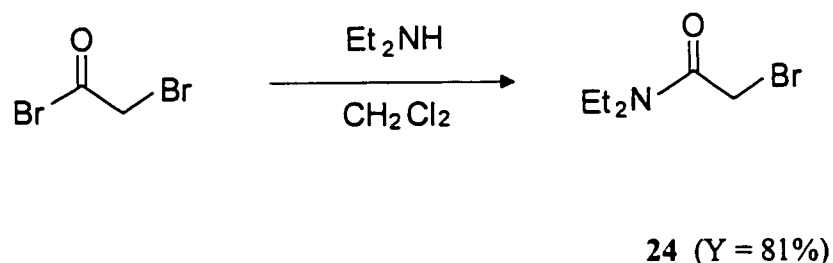


Figure 37. Synthesis of 2-bromo-*N,N*-diethylacetamide.

The octa-functionalized calix[4]resorcinarenes were prepared as a similar procedure for the formation of tetra-functionalized calix[4]resorcinarenes of Ungaro⁸⁰ and McKervey.⁹⁵ A large excess of sodium hydride (64 mole equivalents) as a strong base promoted the reaction between the resorcinarenes and the excess 2-bromo acetate, as shown in Figure 38. The pure **26** was obtained as thick oil after column chromatography on silica gel with a gradient from 0 to 40% methanol in ethyl acetate. The **29** was

obtained by column chromatography on silica gel with a gradient from 50 to 100% ethyl acetate in petroleum ether. The low reaction yield was due to the chromatography process. The yield of **27** was compatible with previous results ($Y = 24\%$) obtained in our group.⁹⁶

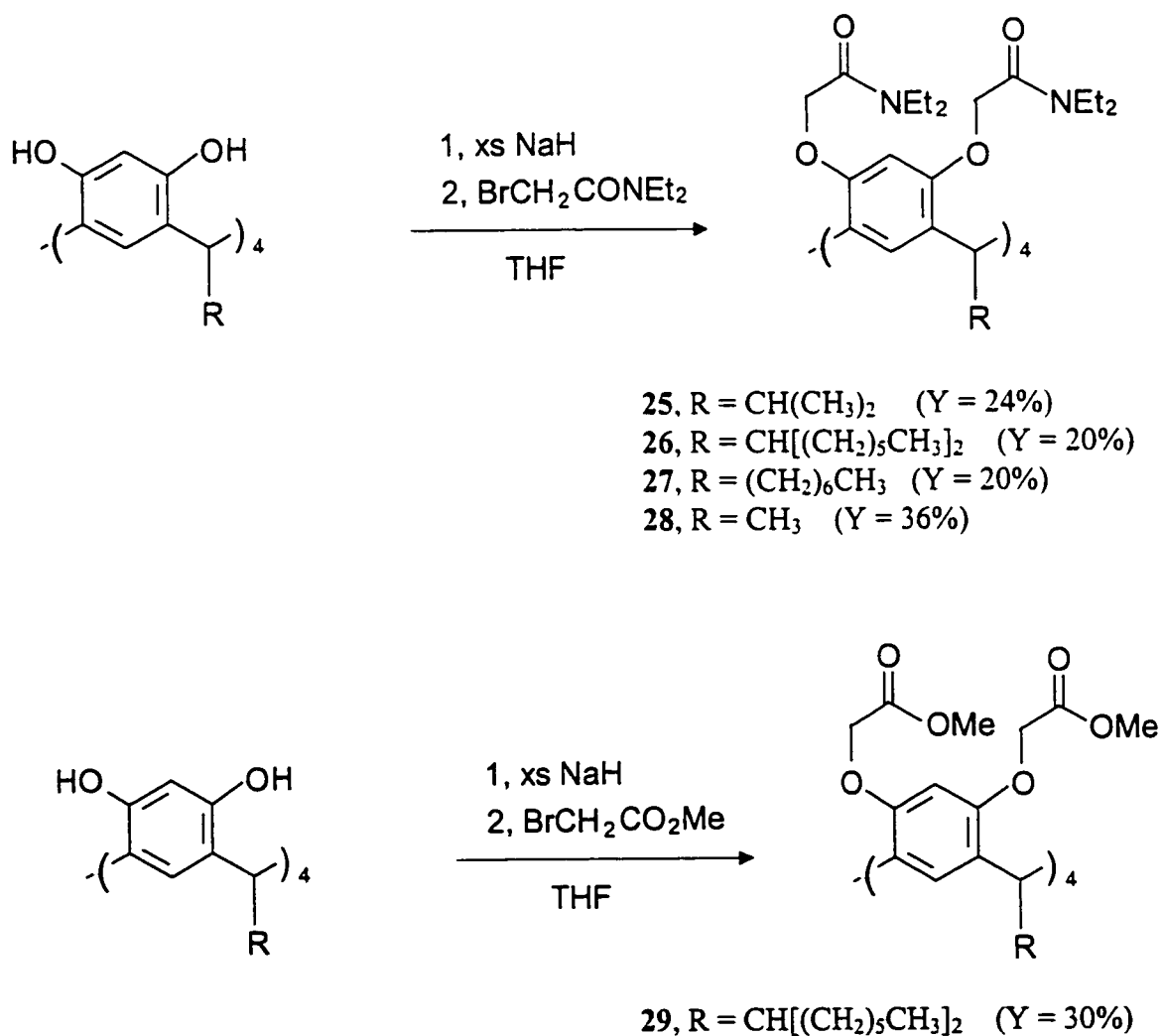


Figure 38. Synthesis of octa-functionalized calix[4]resorcinarenes.

Compounds **25** - **29** were characterized by ^1H and ^{13}C NMR techniques, and the data of the ^1H NMR for these compounds are listed in Table 4. As observed in the resorcinarenes, **21** and **22**, the eight aromatic protons and the four methine protons connected with the tail groups (R) were observed as a single resonance. The protons in the eight carbonyl functional groups $[\text{O}-\text{CH}_2-\text{C}(\text{O})\text{X}]$ were also presented as a single signal. This indicates that like **21** and **22**, the structure of the resorcinarene amide and ester derivatives, **26** and **29** had a four-fold symmetry on the NMR time scale. If a flattened cone conformation is in rapid interconversion with the alternative flattened cone conformation (Figure 39) to be identified on the NMR time scale, an average signal will be observed. Thus, it illustrates that cone conformation and/or flattened cone conformation (a two-fold symmetry) of **26** and **29** are main conformation in solution. Variable temperature NMR technique would be used to prove the flattened cone conformation. These data follow in Section 2.2.

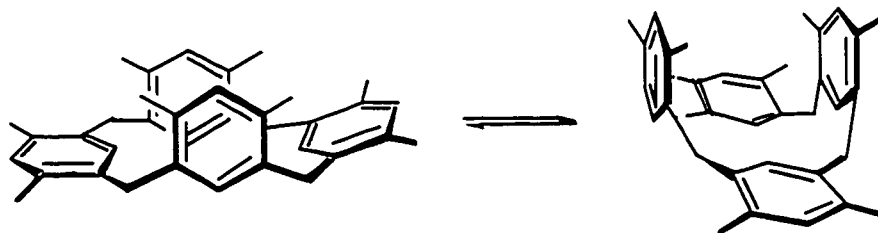


Figure 39. Pseudorotation of flattened cone conformation.

A ^1H NMR spectrum of **26** is shown in Figure 40, which is typical of the octa-functionalized resorcinarenes. The two signals in the region of 6.3 to 6.8 ppm represent the eight aromatic protons. The aromatic protons in the lower rim should be observed in a further downfield than the aromatic protons in the upper rim.⁹⁷

With respect to peak of the upper-rim protons, a broaden peak for the lower-rim protons was explained that the lower-rim protons would be magnetically affected to a greater extent by pseudorotation based on their closer proximity to the anisotropic regions of the adjacent arene rings.

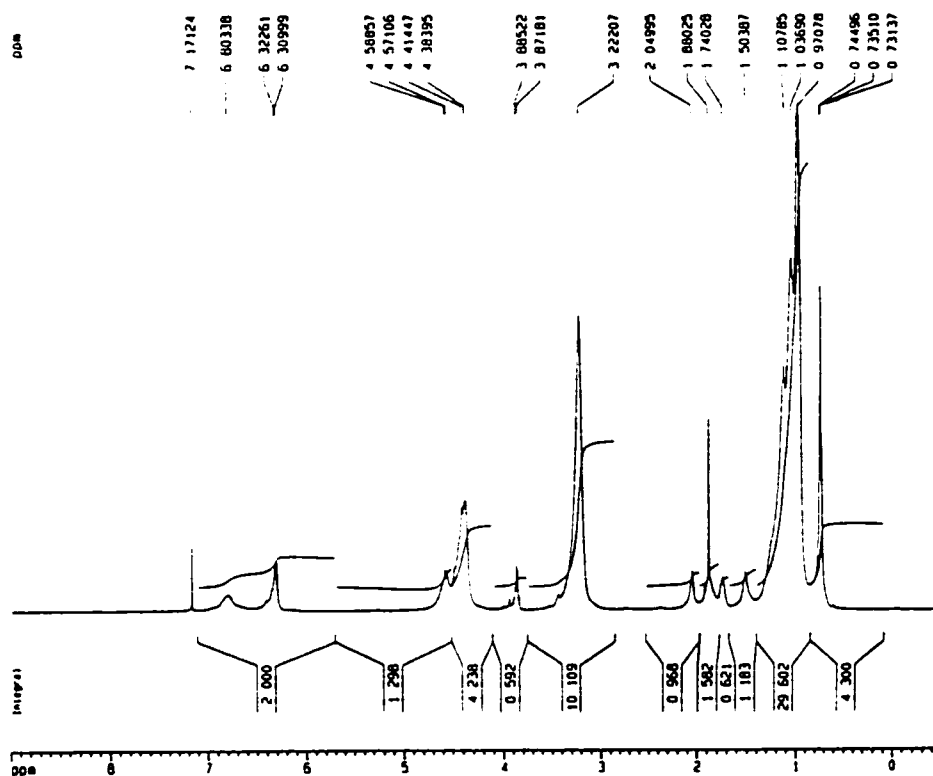


Figure 40. ^1H NMR spectrum of 26.

The slightly broaden signal at 4.59 ppm represents the four methine protons connected with the tail section. Being adjacent to two arene rings the methine protons had anisotropic effect to some extent peak by the pseudorotation. The effect leads to broadening of the peak.

Table 4. The data of ^1H NMR for 25 - 29.

	26	29	25	27	28
functional group	(ppm)				
ArH lower rim	6.80	6.95	6.66	6.81	6.36
ArH upper rim	6.30	6.30	6.45	6.46	6.36
Ar-CH-Ar	4.59	4.42	4.62	4.62	4.60
O-CH ₂ -C(O)X	4.40	4.20	4.52	4.17	4.35
Ar-CH-CH[(CH ₂) ₅ CH ₃] ₂	3.39	3.92	-	-	-
OCH ₃	-	3.67	-	-	-
NCH ₂ CH ₃	3.22	-	3.37	3.44	3.26
Ar-CH-CH(CH) ₃	-	-	2.33	-	-
Ar-CH-CH ₂ (CH ₂) ₄ CH ₃	-	-	-	1.82	-
Ar-CH-CH[CH ₂ (CH ₂) ₄ CH ₃] ₂	1.62	1.85	-	-	-
Ar-CH-CH ₃	-	-	-	-	1.36
Ar-CH-CH ₂ (CH ₂) ₄ CH ₃	-	-	-	1.21	-
NCH ₂ CH ₃	0.98	-	1.05	1.09	1.01
Ar-CH-CH[CH ₂ (CH ₂) ₄ CH ₃] ₂	0.98	1.13	-	-	-
Ar-CH-CH(CH) ₃	-	-	0.85	-	-
Ar-CH-CH ₂ (CH ₂) ₄ CH ₃	-	-	-	0.85	-
Ar-CH-CH[(CH ₂) ₅ CH ₃] ₂	0.74	0.76	-	-	-

The doublet signal at 4.40 ppm is assigned to the sixteen methylene protons of the diethylamide. The doublet signal was also slightly broadened.

The quartlet peak at 3.89 ppm is assigned to the four methine protons at the dihexyl site. The coupling constant, $J = 6.5$ Hz indicates a free rotation of the dihexyl groups.⁹⁸ The remaining signals represent methyl protons of the diethylamides and dihexyl protons in the tail sections.

Compounds **26** - **29** were also characterized by MS analysis. However, neither molecular ion was found, nor any conclusive fragments were identified.

Elemental analysis was used to confirm the synthesized compounds **21**, **22**, **25** - **29**. The elemental analyses of **25**, **27** - **29** were within acceptable value of 0.9% of the calculated values. The elemental analyses of **26** with one molecule of KCl was in agreement with the calculated percentages within the acceptable value. The elemental analyses of **21** with addition of one molecule of H₂O, and **22** with addition of three molecules of HCl were within the accepted values of the calculated percentages.

Once compounds **21** - **29** were synthesized and fully characterized, the next step of the project was to study their characteristics in solution by NMR with varied temperature, and to prepare Langmuir-Blodgett films of these compounds and analyze their spectroscopic characteristics.

2.2. Characterization in Solution

NMR techniques have been widely used in host-guest or receptor-substrate chemistry. A variety of applications of the studies of NMR spectroscopy include determination of the association constants,⁹⁹ the conformation or configuration of

complex,^{80,100} the stoichiometry of host to guest in complex,¹⁰¹ and the thermodynamic parameters of complexation.^{5,102}

Variable temperature ¹H NMR technique was employed to study the conformational interconversion of **26** in solution in the presence and absence of metal cation. The amide derivative **26** as a host molecule and silver ion as a guest were studied in our experiment, because in previous work calix[4]resorcinarene amide derivative exhibited strongest binding ability to silver ion, thus giving a spectrum which would have most pronounced effects due to the binding of the guest. To understand how the host **26** to incorporate the guest in the complex, it is necessary to study the conformations of the free and bound host molecule in the complex.

In order to study the conformation of the free **26** in CD₂Cl₂, variable temperature spectra were collected from ¹H NMR between 180 K and 303 K. Previous work showed the coalescence temperature of tetra-tailed calix[4]resorcinarene amide derivative was about 210 K, and freezing point of deuterated chloroform is not low enough to meet the temperature, deuterated dichloro methane was then chosen as the solvent.

The variable temperature ¹H NMR spectra of **26** in CD₂Cl₂ from 180 to 300 K exhibited that signals of the aromatic protons and the α-amide methylene were broadened at low temperature. The signals of the α-amide methylene protons did not vary as much as previous work. The most notable change in the spectra was the signals of the aromatic protons.

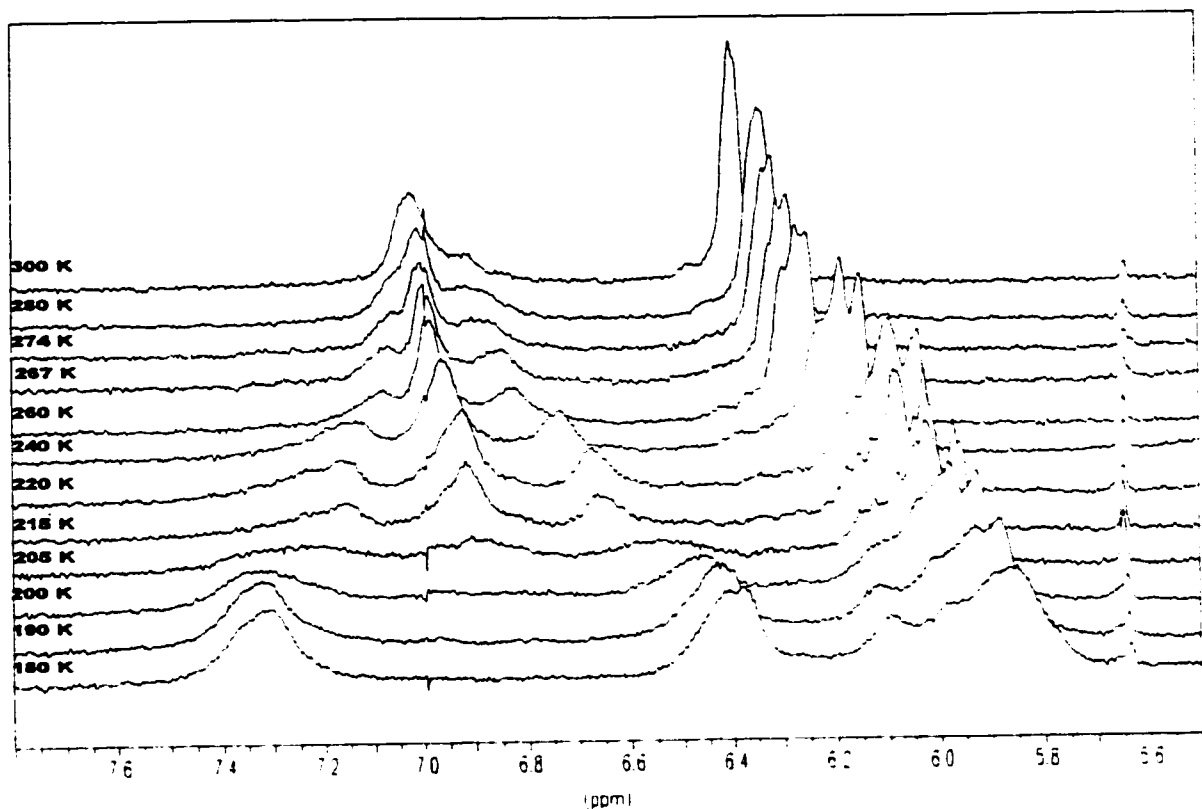


Figure 41. Variable temperature ^1H NMR spectra of aromatic region of **26** in CD_2Cl_2 .

The ^1H NMR spectra of aromatic region of **26** from 180 to 300 K in CD_2Cl_2 is presented in Figure 41. As described in Section 2.1.3, at a temperature of 300 K, signals at 7.01 ppm and 6.40 ppm represents the lower-rim and upper-rim protons, respectively. As the solution was cooled down, the signal at 7.01 ppm was broadened and separated to three signals, and through a coalescence temperature of 210 K, two signals at 7.30 ppm and 6.38 ppm were apparent at the temperature limit of 180 K. The sharp signal of the upper-rim proton at 6.40 ppm was also broadened and separated to two signals at 6.10 ppm and 5.85 ppm as the temperature decreased. The NMR spectra in Figure 42 also displayed some changes in the non-aromatic regions of **26** with varied temperatures.

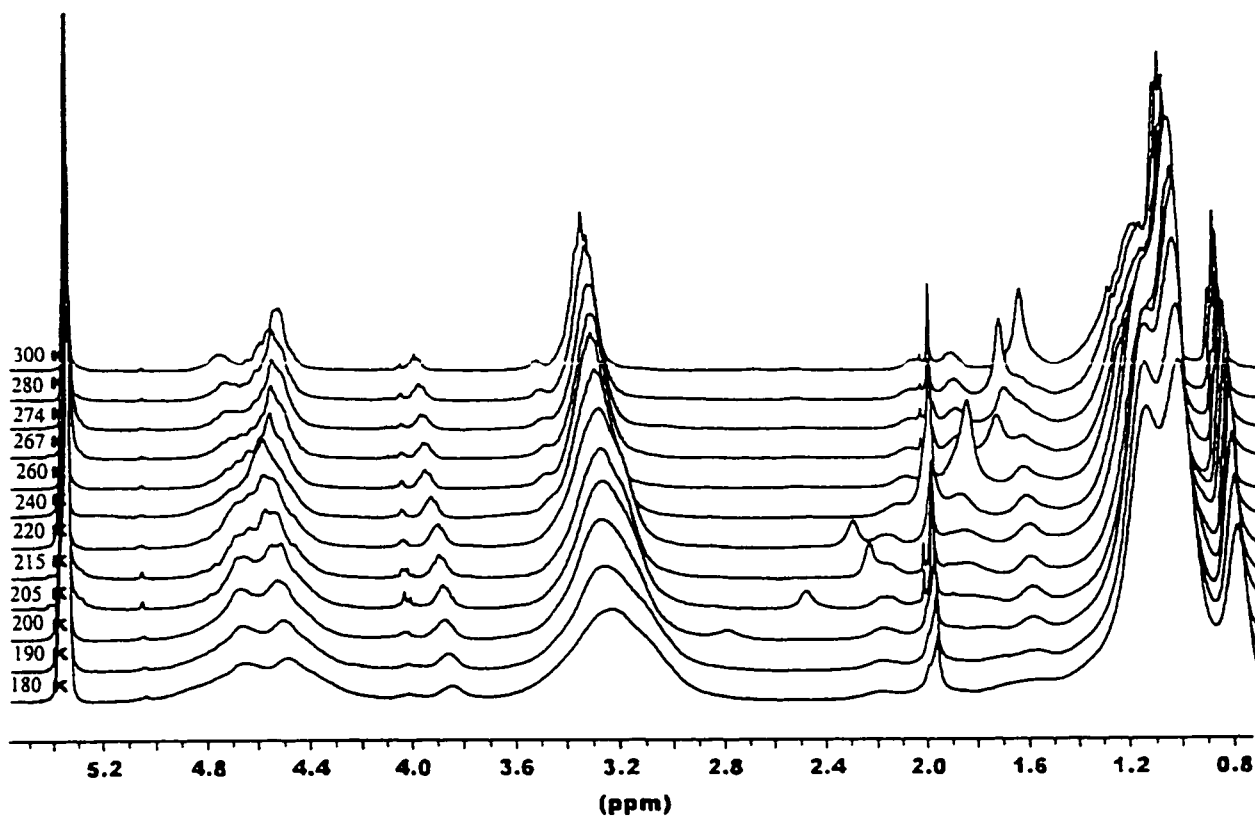


Figure 42. Variable temperature ^1H NMR spectra of the non-aromatic region of **26** in CD_2Cl_2 .

From the four aromatic proton signals at 180 K, the conformation of **26** was determined to be the flattened cone in CD_2Cl_2 . In the slow exchange regime, the pseudorotation of the flattened cone conformer was decreased with respect to the NMR time scale and therefore the signals for the horizontal (H_u' , H_l') and vertical (H_u , H_l) sets of aromatic protons were observed. The presence of four signals rules out the existence of the cone, partial flattened cone, and the 1,3-alternate conformers since these conformations would result in two, six, and two aromatic signals, respectively.

In the pseudorotation of the conformer, the lower-rim aromatic protons undergo a large change in chemical environment, and thus have a larger chemical shift compared to

the upper-rim protons whose chemical environment is only slightly altered. As seen in Figure 43, the lower-rim protons exchange from the vertical plane being deshielded by three rings and shielded by one ring, to the horizontal plane being deshielded by two rings and shielded by two rings. The upper-rim protons are deshielded by one arene ring with some shielding from the opposite parallel ring.

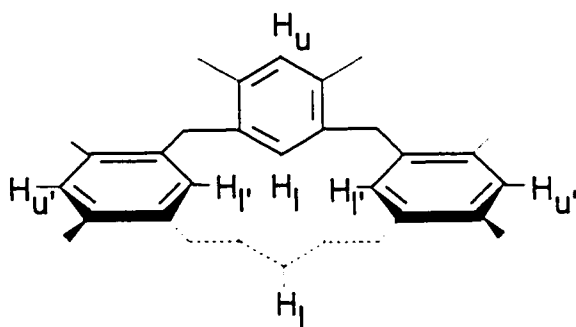


Figure 43. The arene rings and their protons in the flattened cone.

From the coalescence absolute temperature (T_c) and the difference between the two signals ($\Delta\delta$), the exchange rate (k_c) at the coalescence temperature was determined from Equation 1. The free energies of activation (ΔG^\ddagger) at the coalescence temperature for **26** were determined from Equation 2,¹⁰³ where h is Plank's constant and k_B is Boltzmann's constant.

The free energies of activation for **26** in CD_2Cl_2 are listed in Table 5 for the aromatic protons, the α -amide methylene protons and the nearest methylene protons in the tail alkyl chains.

$$k_c = \frac{\pi\Delta\delta}{\sqrt{2}} \quad \text{Eq. 1}$$

$$\frac{-\Delta G^\ddagger}{RT_c} = \ln \frac{k_c h}{k_B T_c} \quad \text{Eq. 2}$$

Our observation indicates **26** existed as rapidly equilibrating conformer in solution. It is consistent with the observation from *C*-undecylcalix[4]resorcinarene amide derivative, but it is different from cone conformer of parent calix[4]resorcinarene in which hydrogen bonding between the eight hydroxy groups of the upper-rim. The activation energy was about 39.9 kJ/mol in our experiment. This value was compatible to the activation energy of 42.3 kJ/mol from *C*-undecylcalix[4]resorcinarene amide derivative.⁴⁶

Table 5. The free energy of activation of **26 and coalescence temperature.**

ΔG^\ddagger (kJ/mol)	T_c (K)	δ (ppm)
40.5	215	1.60, 2.18
41.6	210	4.50, 4.68
37.6	204	6.40, 7.32
40.0	205	6.10, 5.85
39.9 (Average)		

The presence of silver ion in solution had an effect on the ¹H NMR spectra of **26**. Silver ion was chosen as guest ion since the calix[4]resorcinarene amide derivative had a highest binding constant to it.⁴⁹ Figures 44(a) and (b) are the ¹H NMR spectra of free **26**

and bound **26** in CD_2Cl_2 at 303 K, respectively. The two peaks for the aromatic protons of free **26** were broadened when silver ion was present in CD_2Cl_2 solution. This is a result of the complexation between carbonyl oxygens of **26** and silver ion, which slows down the interconversion rate of the flattered cone conformations.

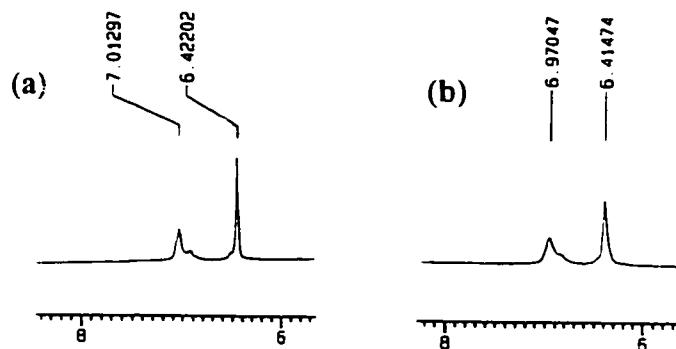


Figure 44. Comparison of ^1H NMR spectra of arene region of (a) **26** and (b) $26 \bullet \text{Ag}$ in CD_2Cl_2 .

The variable temperature ^1H NMR of $26 \bullet \text{Ag}^-$ in CD_2Cl_2 was performed from 303 K to 244 K (Figure 45). Two signals of the aromatic protons at 6.97 ppm and 6.41 ppm were broadened as the solution temperature decreased. The signal at 6.97 ppm was separated to two signals through a coalescence temperature. The coalescence temperature was estimated as 268 K. The calculated activation energy of bound **26** was 51.1 kJ/mol that was higher than free **26** as we expected. The upper-rim proton signal was not separated as the temperature decreased, which was different from the free **26** case. This could be as a result of the complexation slowing down the pseudorotation and a smaller chemical environment altered at the upper-rim protons than the lower-rim.

The signals for the non-aromatic region of **26** complexed with silver ion were broadened when the solution temperature decreased. Especially, the α -amide methylene signal was overlapped with the methine connected with the tail section at about 268 K. There was no coalescence temperature exhibited as the temperature cooled down.

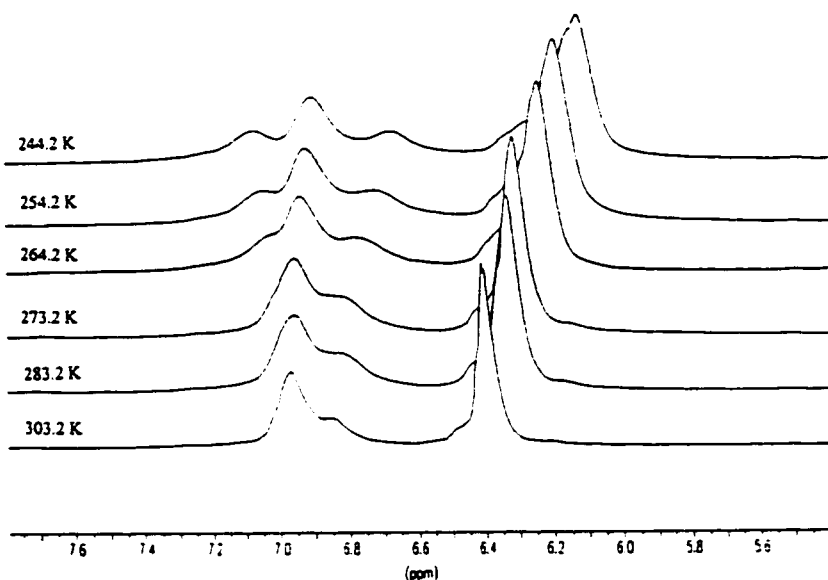


Figure 45. Variable temperature ^1H NMR spectra of aromatic region of $26 \cdot \text{Ag}^+$ in CD_2Cl_2 .

2.3. Behavior of Langmuir-Blodgett Films

Langmuir-Blodgett (LB) films are well-ordered two dimensional solids.⁶⁷ The conformational changes of calix[4]resorcinarenes, which were observed in solution would be restricted in the LB films. Previous work in our laboratory reported various metal ions incorporated into the LB films of resorcinarene ester and amide derivatives.^{84,85} The LB technique offers a suitable environment to study the molecular orientation and interactions in the solid state.

2.3.1 Langmuir Monolayer Properties

The characteristics of the surface pressure-area (π - A) isotherm have been used to analyze the behavior of the Langmuir films of several materials at the air-water interface. The limiting area is estimated from the intercept by extrapolating the linear region (liquid-condensed phase) to zero surface pressure in the isotherm. As example, limiting area ($A = 1.16 \text{ nm}^2$) for *C*-methylcalix[4]arene was in agreement with the area of the upper rim of cone-shaped calixarene cavity estimated by X-ray data.⁷⁶ The Langmuir film collapse pressure is recorded when the slope of the surface pressure to molecule area in the isotherm deviates from the linear relationship. When the film collapses, it was believed that the monolayer is changed to disordered multilayers, in which the molecular layers are riding on top of each other.⁶⁸

In the preparation of Langmuir monolayer of $2 \times 10^{-4} \text{ M}$ of **21** - **29** which were dissolved in organic solvent, the solvent was spread on the aqueous subphase at 15°C or 25°C . After waiting 30 min for solvent evaporation and equilibration of the interaction of the compounds with the subphase, the barrier movement was initiated and the π - A isotherms were recorded.

The π - A isotherms of **21** - **29** were obtained from 10% methanol/chloroform solution. 10% methanol/toluene as solvent was also used to obtain the isotherm of **21**, and it was not used for other compounds due to the toluene exhibiting a strong influence on limiting area in the isotherm (Figure 49). The methanol/chloroform solvent mixture was required to improve the solubility of the resorcinarenes. The reproducible π - A isotherms of the above compounds were obtained in our experiments.

The π - A isotherms of **22** from 10% methanol/chloroform solution exhibited that when the subphase temperature increased from 15°C to 25°C the limiting area of 1.42 nm² (Figure 46) decreased to 1.25 nm² (Figure 47). A liquid-expanded to liquid-condensed transition region⁶⁷ was observed at 25°C, but not manifested at 15°C. Thus, the intercept (limiting area) obtained by extrapolating the liquid-condensed region to zero surface pressure became smaller at 25°C compared to at 15°C. The liquid-expanded to liquid-condensed transition was also manifested in the π - A isotherm of **23** at 25°C. The similar observation was reported in previous work that the limiting areas of *C*-undecylcalix[4]resorcinarene in toluene solution vary from the temperatures of 15°C and 25°C.⁸⁴ This indicates the molecule packing behavior in the Langmuir monolayer varies with temperature. It seems that there is a lack of ability of “liquid” to reorganize at the lower temperature as the surface pressure is increased.

The π - A isotherm obtained from different spreading solvents exhibited different the limiting areas. The π - A isotherm of **21** showed the limiting area of 0.76 nm² from 10% methanol/chloroform solution in Figure 48 and the limiting area of 1.25 nm² from 10% methanol/toluene solution in Figure 49. Reinhoudt¹⁰⁵ reported that the conformational distribution of calixarenes is strongly influenced by the solvent, and that the inclusion of solvent molecules into the cavity of calixarenes takes place. Cram³³ has pointed out that chloroform interacts with the bowl-shaped cavity of cavitands by the insertion of one chlorine atom and that toluene is bound through the methyl group. The increase in the limiting area we observed when using toluene may be due to the inclusion of the methyl group of toluene with a larger cross-sectional area than the chlorine atom

into the cavity of the calix[4]resorcinarene in the Langmuir films. The toluene molecule might be also inserted between two resorcinarene molecules through $\pi - \pi$ interaction to contribute the limiting area increase.

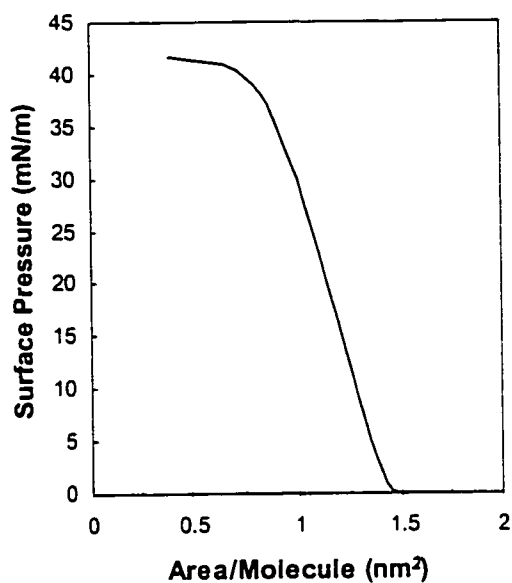


Figure 46. Surface pressure-area isotherm of 22 at 15°C.

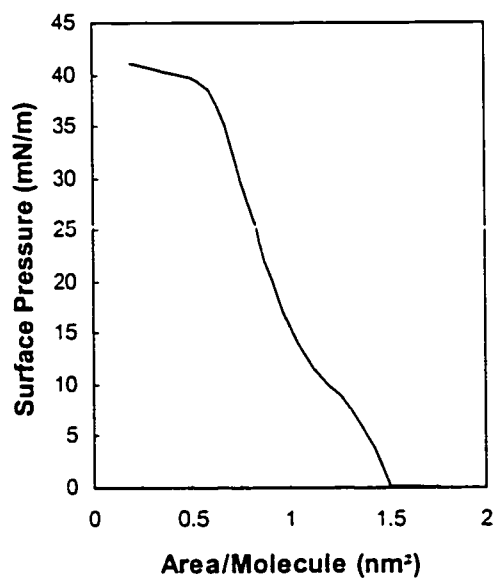


Figure 47. Surface pressure-area isotherm of 22 at 25°C.

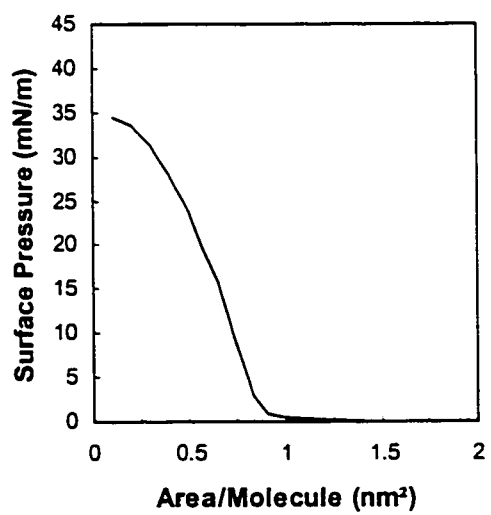


Figure 48. Surface pressure-area isotherm of 21 from 10% methanol/chloroform solution.

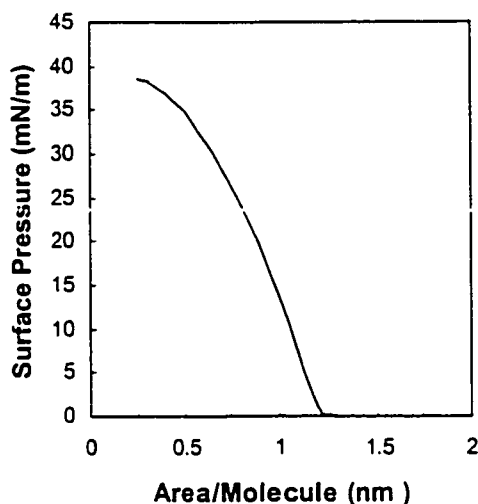


Figure 49. Surface pressure-area isotherm of 21 from 10% methanol/toluene solution.

Table 6 presents the limiting areas and collapse pressures of 21 - 29 from 10% methanol/chloroform solution at 25°C. From a thermodynamic point of view, the association equilibrium for the interaction between metal cations and the monolayer would be favored at higher temperature. For this reason the π -A isotherms were obtained at temperature of 25°C.

As expected, in Table 6 the amide derivatives 25 - 28 had larger limiting areas on the monolayers than the ester derivative 29. Also, the amide derivatives, 26 and 27 and ester derivative 29 exhibited larger limiting areas with respect to the parent resorcinarenes 21 and 22. This illustrates the functional groups were responsible for the difference in the limiting area. In the Langmuir films at air-water interface, the hydrophilic functional

groups such as amide, ester and hydroxy were extended into the aqueous subphase and the hydrophobic tail alkyl chains were lifted away from the aqueous surface.

Table 6. The limiting area and collapse pressure of 21 - 29 from 10% MeOH/CHCl₃ at 25°C.

Compound	Limiting area (nm ²)	Collapse pressure (mN/m)
21	0.76	32
22	1.25	36
22*	1.50	36
23	1.00	28
23*	1.55	32
25	2.75	23
26	2.80	32
27	2.50	36
28	3.30	17
29	2.00	28

* Temperature of the subphase: 15°C.

Moreover, the structure of the tail alkyl chains also has an effect on behavior of the Langmuir films. *C*-methylcalix[4]resorcinarene amide derivative (**28**) has a largest limiting area in the compressed monolayer from 10% methanol/chloroform solution at

25°C, compared to those of other amide derivatives, **25** - **27**. This illustrates that the alkyl chain structure such as length and cross sectional area of the alkyl chains greatly influences the limiting area in the monolayer. The larger limiting area of **28** indicates its amide groups extended into the aqueous subphase to greater degree, because of relatively weak hydrophobicity of the short-tail methyl chains to lift into the air. The branched alkyl chains (larger cross sectional area) in **27** and long alkyl chains in **25** and **26**, have strong hydrophobicity and prevent the hydrophilic amide groups to further extending.

The limiting area of the octa-tailed resorcinarene (**22**) was slightly larger than the tetra-tailed resorcinarene (**23**), but much smaller than the amide and ester derivatives **25** - **29**. Unlike theoretical calculation, the modification of the tetra-tailed alkyl chains to octa-tailed alkyl chains did not greatly increase the limiting area of the parent calixresorcinarene (**22**). The limiting area of **22** ($A = 1.25 \text{ nm}^2$) was smaller than the theoretical data of the eight methylene chains ($A = 1.92 \text{ nm}^2$). This might be due to aggregation of the eight alkyl chains in the Langmuir films. In the case of the limiting area of **22**, the limiting area value at 2.38 nm^2 was observed, but it was not possible to obtain the reproducible isotherm under our experimental conditions.

With the same alkyl tails, the amide derivative, **26** exhibited the collapse pressure of 32 mN/m and the ester derivative, **29** exhibited the collapse pressure of 28 mN/m from 10% methanol/chloroform solution. When the monolayer collapsed the molecular layers lift from the water subphase. The difference in the collapse pressure indicates that the hydrophilic amide groups of **26** had a stronger interaction with the water than the ester groups of **29**.

Table 6 also clearly presents that **21 - 23, 26, 27, 29** with longer alkyl chains in the tail section exhibited a higher collapse pressure than **25** and **28** with a short tail section. The collapse pressure varied from the solubility of these materials. The length of the tail alkyl chains may have an effect on the molecular arrangement on the Langmuir films. At the air-water interface, the longer tail alkyl chains the film-forming molecules contain, the better the film-forming molecules pack as the surface pressure increases. This observation is consistent with previous work for CALOL, CALAM and CALES, in which their collapse pressure was up to 40 mN/m.^{84,85}

2.3.2 The Characteristics of Langmuir-Blodgett Films

Metal ions incorporated into well-ordered multilayers (LB films) can be transferred onto substrates by LB deposit technique. Previous work has already shown terbium ion (Tb^{3+}) encapsulated into *C*-undecylcalix[4]resorcinarenes in LB film based on their spectral properties.⁶² Therefore, the LB films hold great promise for the development of molecular sensors.

C-undecylcalix[4]resorcinarene amide derivative showed a strongest binding ability towards silver ion (Ag^+) based on logarithm of association constant.⁴⁶ Thus, in our project the Ag^+ was selected as metal ion for incorporation with the octa-tailed calix[4]resorcinarenes in the LB film.

The LB films complexed with Ag^+ were transferred onto quartz at a temperature of 25°C. The monolayer of **26** in liquid-condensed phase was at surface pressure of 28

mN/m, thus efficient transfer (transfer ratio $\tau = 1$) of the floating films on quartz was performed at 28 mN/m where the monolayer was well packed.

A single LB film (01 LB, monolayer LB film on each side of the substrate) was obtained on quartz from **26** complexed with Ag^+ ($\mathbf{26}\bullet\text{Ag}^+$) in 10% methanol/chloroform solution at 25°C. The single monolayer LB film of $\mathbf{26}\bullet\text{Ag}^+$ on quartz substrate were prepared from 2×10^{-4} AgNO_3 subphase. The quartz slide started in the downward direction and there was not layer transferred onto the slide. The first LB film was transferred from the $\mathbf{26}\bullet\text{Ag}^+$ solution onto the quartz slide in the upward direction. This type of transfer orients the amide head group complexed with Ag^+ towards the quartz surface and the hydrophobic alkyl tail section away from the surface, in a Z-type deposition (Figure 12). The second LB film was not transferred onto the quartz on the subsequent downstroke, instead, the first LB film on the quartz came off ($\tau = 0$) on the downstroke. This illustrates the second layer could not be deposited as tail-to-tail fashion with the first layer. It might indicate the hydrophobic-hydrophobic interaction of the two layers was not compete effectively with the interaction of the hydrophilic head group with the water subphase.⁶² In addition, it was not possible to form multilayer LB film of $\mathbf{26}\bullet\text{Ag}^+$ on quartz even at 15°C. Our observation indicates the modification of the tetra-tailed section to octa-tailed section did not improve the interaction between the hydrophobic-hydrophobic alkyl chains enough to form multilayers on quartz.

However, a 10-layer LB film (10 LB, 10-layer LB film on each side of the substrate) was obtained on quartz from **29** complexed with Ag^+ ($\mathbf{29}\bullet\text{Ag}^+$) in 10% methanol/chloroform solution at 25°C. The Langmuir film of **29** was transferred onto the

quartz at surface pressure of 25 mN/m where the film was in liquid-condensed region. Unlike previous work,⁸⁴ these ten layers were always transferred onto the quartz slide on the upstroke of the dipping device. It was not possible to transfer the layers onto the quartz on the downstroke. This type of transfer orients the head group complexed with Ag^+ towards the quartz surface in the first layer, and the head group with Ag^+ in the second layer orients towards the tail section of the first layer. Thus, the 10-layer LB film was fabricated in a head-to-tail fashion. Formation of the multilayers of **29** in air-water interface indicates that the ester head groups of **29** has a weak interaction with the water subphase compared to the amide head groups of **26** and a relatively strong interaction between the hydrophilic ester groups and the hydrophobic alkyl groups.

The above observations are different from the results of CALOL and CALES. The multilayer LB films of CALOL and CALES were obtained on the downstroke⁸⁴ and the formation was in a tail-to-tail fashion. This structure indicates a relatively strong interaction between the tails as result of their longer tail alkyl chains and better package compared to **29**. Aromatic compound with long alkyl chain was likely to form multilayers in X-type deposition (tail-to-tail) and aromatic compound with short alkyl chain was likely to form multilayers in Z-type deposition (tail-to-head). However, it is unclear at this time the exact nature of the interaction between the hydrophilic groups and the water, interaction between hydrophobic (tail) and hydrophilic (head) groups and hydrophobic and hydrophobic groups or hydrophilic and hydrophilic groups.⁶²

2.4. Characterization in Langmuir-Blodgett Films

In order to completely understand the interaction between calixresorcinerene and metal ions in LB films, it is necessary to study the conformation of the calixresorcinarene incorporated with metal ions. As described above in solution one flattened cone conformation of the resorcinarene was interconverted with the alternative flattened cone conformation. In the solid-like LB films the conformation may be different from that in solution.

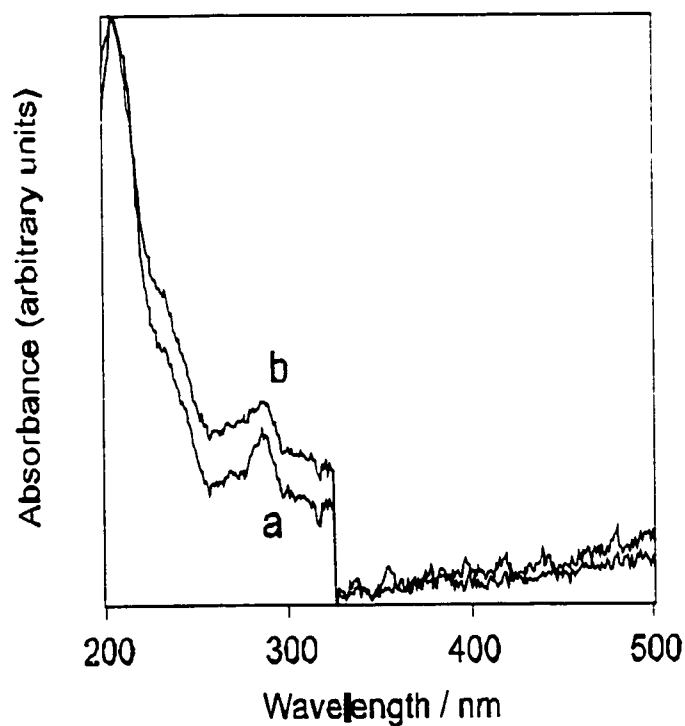


Figure 50. UV-visible spectra of 01 LB of (a) 26 and (b) 26•Ag⁺.

Figure 50 shows the UV-visible spectra of monolayer LB film of **26**. The UV-visible spectra (Figure 50a and b) are the LB films on quartz obtained from pure aqueous subphase and aqueous subphase containing Ag^+ . The spreading solvent was 10% methanol/chloroform solution at 25°C. There were two absorptions observed in the UV region centered at 286 nm and 247 nm. The absorptions at 286 and 247 nm were assigned to two different conformations in LB film, cone (C_{4v}) and flattened cone (C_{2v}), respectively, based on the study of distinctly different adsorptions at 286 nm from toluene and at 247 nm from chloroform.⁸⁴ This indicates that **26** existed in the cone and flattened cone conformation in the LB film. In the flattened cone conformation two of the benzene rings disposed across the macrocycle from one another are approximately parallel to the aqueous subphase surface and the other two are approximately perpendicular.⁸⁵ It is hard to point out which conformation was preponderant since the 247 nm band rose into the allowed $\pi - \pi^*$ transitions.

The UV-visible spectrum of LB films of **26** from aqueous subphase containing silver ion was similar to the **26** taken from pure aqueous subphase. The presence of silver ion in the aqueous subphase did not cause the conformation change in the LB films. It is consistent with the observation for the tetra-tailed resorcinarene derivative, CALAM.⁸⁵

Both cone and flattened cone conformations present in the LB film are different from the observations for the tetra-tailed resorcinarenes (CALAM and CALES), which only exhibited flattened conformation (247 nm) in the LB films.⁸⁴ The difference might be due to the modification of the tetra-tailed to the octal-tailed. A larger cross sectional

area of the octa-tailed makes possible to form cone conformation at the head groups in Langmuir films.

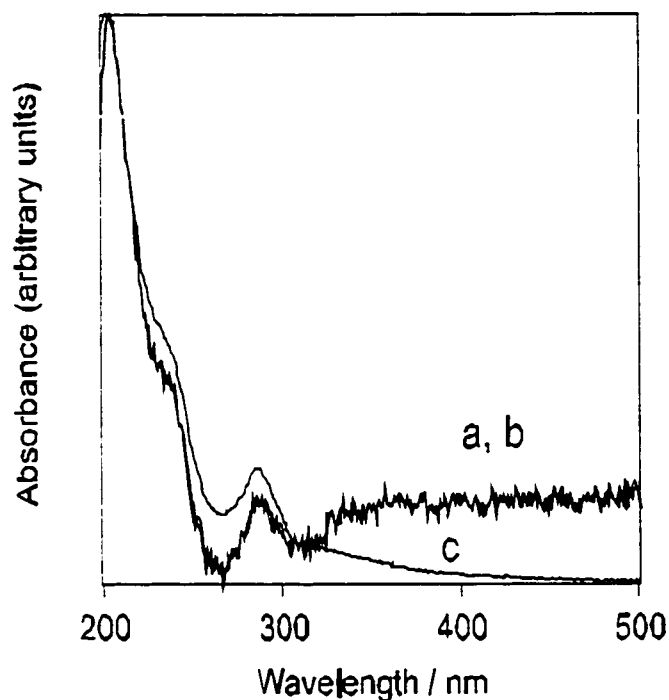


Figure 51. UV-vis spectra of 01 LB of (a) 29 and (b) $29 \bullet Ag^+$ and 10 LB of (c) $29 \bullet Ag^+$.

UV-visible spectra in Figure 51a, b and c are monolayer LB film of 29, monolayer LB film of 29 incorporated with silver ion ($29 \bullet Ag^+$) and 10-layer LB films of $29 \bullet Ag^+$ on quartz, respectively. Two absorption bands at 286 nm and 247 nm were observed in the three cases. Both cone and flattened cone conformations were present in the LB films. The fact that the spectrum (Figure 51a) of 29 obtained from an aqueous subphase containing silver ion is identical to the spectrum (Figure 51b) from pure aqueous

subphase illustrates that the addition of Ag^+ in the subphase did not have effect on the conformation of **29** in the LB films. As we expected, in the UV-visible spectrum (Figure 51c) 10-layer LB films of $\text{29}\bullet\text{Ag}^+$ showed much stronger absorption bands at 286 and 247 nm than the monolayer LB film of $\text{29}\bullet\text{Ag}^+$. The observation confirms that the multilayer LB films were successfully transferred onto quartz from the aqueous subphase containing silver ion, and the conformations of **29** in the floating monolayer were not modified during the transferring process.

2.5 Conclusion

The octa-tailed resorcin[4]arenes, **21** and **22**, and the resorcinarenes functionalized with pendant α -(diethyl acetamide), **26** or α -(methyl acetate), **29** were synthesized. Compound **22** was prepared by the cyclooligomerization of resorcinol and α,α -dihexyl acetaldehyde under acid-catalyzed conditions with 20% yield. Good yields of α,α -dihexyl acetaldehyde were obtained through the reaction of dihexyl ketone with a phosphonate reagent. Subsequently, **22** was functionalized using 2-bromo-*N,N*-diethyl acetamide) or methyl bromoacetate under basic conditions.

With the help of variable temperature ^1H NMR technique, the flattened cone conformation of the functionalized resorcinarenes was determined in solution. The functionalized resorcinarene acting as a host molecule incorporated with silver ion was also given a flattened cone conformer for the metal complex. The free energies of activation were calculated from the coalescence temperature for the pseudorotation of the free host **26** and bound **26** in CD_2Cl_2 .

Langmuir films and LB films of the octa-tailed resorcinarenes and their amide and ester derivatives were fabricated at the water/air interface. The π - A isotherm varied with a change in the spreading solvent, subphase temperature and the resorcinarene structure. When toluene was used as spreading solvent, it significantly affected the limiting area of the resorcinarene relative to chloroform. A smaller limiting area was observed at 25°C compared to 15°C as a result of more defined liquid-condensed region exhibited at 25°C. As expected, the modification of four tail chains to eight tail chains of the resorcinarene increased approximately 20% in the limiting area, but it was not large enough to meet the limiting area of the amide or ester derivatives.

One-layer LB film of **26** incorporated with Ag^+ was obtained on quartz. It was not possible to form multilayer LB film of $\text{26}\bullet\text{Ag}^+$ on quartz. Ten-layer LB film of $\text{29}\bullet\text{Ag}^+$ was fabricated on quartz. The multilayer LB film was transferred onto the substrate when the substrate was in the upward direction, and believed to be in a head-to-tail fashion.

Unlike in solution and the tetra-tailed resorcinarenes, **26** and $\text{26}\bullet\text{Ag}^+$ were present as both cone (C_{4v}) and flattened cone (C_{2v}) conformers in the solid-like LB film according to absorption bands at 286 nm and at 247 nm in UV-visible spectra of the monolayer LB films. **29** and $\text{29}\bullet\text{Ag}^+$ also present as cone and flattened cone conformers in monolayer LB film and 10-layer LB films which exhibited much stronger absorption intensity in UV-visible spectra than the monolayer LB film.

3. EXPERIMENTAL

3.1 General Procedures/Instruments

Nuclear magnetic resonance (NMR) spectra were recorded on an Avance Bruker AC Spectrometer at 300 or 500 MHz for ^1H and 75 or 125 MHz for ^{13}C . The low temperature experiments were performed using a Bruker Variable Temperature Unit. Chemical shifts are reported in ppm on the δ scale using the solvent line relative to Me_4Si as an internal standard. Infra-red spectra were run on Bomem Michelson 100 and recorded with Win-Bomem. Liquid samples were performed as neat films on potassium bromide plates, and solid samples run as pellets in potassium bromide powder. Mass spectrometry was performed on a high resolution, double focusing mass spectrometer. UV-visible absorption spectra were obtained on a Response UV-visible Spectrophotometer interfaced to an IBM PC in a wavelength range of 200 to 500 nm. Elemental analyses were performed by Galbraith[®] Laboratories, Inc., Knoxville, Tennessee. The melting points were determined on a Fisher-Johns hot plate melting point apparatus and were not corrected. Column chromatography was performed using silica gel 60 (70-230 mesh) and thin layer chromatography (TLC) was carried out on Merck aluminum backed plates coated with 0.2 mm silica gel 60 with 254 nm UV indicator. Spots were visualized under UV light or with dip solution.

3.2 Materials

All chemicals were purchased from Aldrich or from BDH and were of ACS reagent grade. Most chemicals were used without further purification unless noted.

Tetrahydrofuran (THF) was distilled from sodium and benzophenone ketyl. Dichloromethane was distilled from calcium hydride. 1,2-Dihydropyran and isobutyraldehyde were both distilled under a dry nitrogen atmosphere immediately prior to use.

Diethyl[(2-tetrahydropyranyloxy)methyl]phosphonate (18)⁹¹

Paraformaldehyde (5.93 g, 197 mmol) and triethylamine (1.96 g, 19.4 mmol) were added into a 250-mL round bottom flask under stirring, and then diethyl phosphite (27.3 g, 198 mmol) was added. The mixture was heated at 120°C for 12 hrs, and then evaporated at 60°C under reduced pressure for 2 hrs. Diethyl ether (100 mL), freshly distilled 1,2-dihydropyran (16.4 g, 195 mmol) and phosphorus oxychloride (10 drops) were added to the above mixture which was stirred at room temperature for 30 min. Another part of the dihydropyran (8 g) and phosphorus oxychloride (5 drops) was then added. The reaction solution was stirred for 4 hrs. When TLC (50% ethyl acetate/petroleum ether) showed the reaction to be completed, the mixture was diluted with diethyl ether (200 mL), and then was washed with 5% sodium bicarbonate solution (50 mL) and brine (50 mL). After being separated the ether layer was dried over anhydrous magnesium sulfate and evaporated under reduced pressure to give a slightly yellow oil (40.5 g). This crude material was purified by column chromatography using 50% ethyl acetate/petroleum ether to give pure compound 18 as a colorless oil (36.4 g, 76%, $R_f = 0.15$ in ethyl acetate).

$^1\text{H NMR}$ (CDCl_3): 4.63 (t, 1H, $J = 2.8\text{Hz}$), 4.12 (m, 4H), 3.93 (q, 1H), 3.73 (q,

1H), 3.65(q, 1H), 3.45 (m, 1H), 1.58 (m, 6H), 1.67 (t, 6H, J = 7.1Hz).

¹³C NMR (CDCl₃): 99.1, 62.4, 61.5, 59.3, 29.9, 25.2, 18.6, 16.4.

2-Hexyl-octenyl 2-tetrahydropyranyl ether (19)

Diisopropylamine (420 mg, 4.00 mmol) and THF (200 mL) were added into a 3-neck 500 mL round bottom flask under a nitrogen atmosphere. The solution was cooled to -78 °C in an acetone/CO₂ bath. A hexane solution of *n*-butyllithium (2.90 mL, 1.40M, 4.06 mmol) was added at once by a syringe. The above phosphonate **18** (1.00 g, 3.96 mmol) was added into the mixture solution over 2 min via a syringe. Dihexyl ketone (674 mg, 3.30 mmol) in THF (20 mL) was added dropwise from a constant addition funnel. After completing the addition the dropping funnel was replaced with a reflux condenser, and the cooling bath was replaced with a heating mantle. The mixture was heated to reflux overnight. The mixture was diluted with diethyl ether (200 mL), and then was washed in turn with hydrochloric acid (10%, 20 mL), water (50 mL) and saturated sodium bicarbonate solution (50 mL). After being separated the ether layer was dried over anhydrous magnesium sulfate and evaporated under reduced pressure to give a slightly yellow liquid, and further purification was carried out by column chromatography with 2% ethyl acetate/petroleum ether to give pure compound **19** as a colorless liquid (580 mg, 68.2%, R_f = 0.7 in 5% ethyl acetate/petroleum ether).

¹H NMR (CDCl₃): 6.00 (s, 1H), 4.82 (t, 1H, J = 3.0Hz), 3.78 (m, 1H), 3.53 (m, 1H), 2.08 (t, 2H, J = 7.1Hz), 1.85 (t, 2H, J = 7.4Hz), 1.61 (m, 6H), 1.29 (m, 16H), 0.85 (m, 6H).

^{13}C NMR (CDCl_3): 137.5, 120.1, 98.3, 61.9, 32.0, 30.1, 29.5, 28.3, 27.0, 25.5,
22.8, 19.0, 14.3.

IR (cm^{-1}): 2926 br s, 2729 w, 2666 w, 1730 s, 1680 s, 1455 s, 1354 m, 1202 m,
1037 m.

MS: (EI): M^+ , 296; $\text{M} - [\text{CH}_3(\text{CH}_2)_5]_2\text{CH}=\text{CH}-\text{O}$, 85.

α,α -Dihexyl acetaldehyde (20)

The above enol ether 19 (5.63 g, 19.0 mmol) was dissolved in THF (50 mL) in a 500 mL 3-neck round bottom flask with a magnetic stirrer under a nitrogen atmosphere, and water (200 mL) was slowly added until the solution became turbid. Concentrated hydrochloric acid (6.50 g, 64.0 mmol) was added at once via a syringe. The mixture was heated at reflux for 24 hrs, and the reaction solution was mixed with saturated sodium bicarbonate solution (3 x 50 mL), and extracted with diethyl ether (300 mL). The ether layer was dried over anhydrous magnesium sulfate and evaporated under reduced pressure to give a crude material (4.03 g). Further purification was carried out by column chromatography with 5% ethyl acetate/petroleum ether to give pure compound 20 as a colorless oil (3.14 g, 78%, $R_f = 0.4$ in 5% ethyl acetate/petroleum ether).

^1H NMR (CDCl_3): 9.56 (d, 1H, $J = 3.1\text{Hz}$), 2.23 (s, 1H, $J = 2.7\text{Hz}$), 1.61 (m, 2H),
1.42 (m, 2H), 1.28 (s, 16H), 0.88 (t, 6H, $J = 6.6\text{Hz}$).

^{13}C NMR (CDCl_3): 205.9, 52.2, 31.8, 29.6, 29.1, 27.2, 22.8, 14.2.

IR (cm^{-1}): 2928 br s, 2692 m, 1728 s, 1465 s, 1378 m, 1183 m, 724 m.

MS: M^+ , 212; $\text{M} - \text{CH}_2\text{O}$, 182.

Tetra(*C*-isopropyl)calix[4]resorcinarene (21)

Resorcinol (5.00 g, 45.4 mmol) was dissolved in anhydrous ethanol (150 mL) in a 250 mL 3-neck round bottom flask with a magnetic stirrer, and isobutyraldehyde (3.27 g, 45.4 mmol) was added under a nitrogen atmosphere. The reaction mixture was cooled to 0°C in an ice bath and concentrated hydrochloric acid (22.3 g, 226 mmol) was added slowly. After completing the addition, the ice bath was replaced with heat mantle, and the mixture was heated up to 70°C for 24 hrs. Upon cooling, water (100 mL) was added to promote precipitation. The precipitant was filtered and evaporated under reduced pressure to afford a yellow-brown solid (4.38 g) which was recrystallized from a mixture of cyclohexane and ethyl acetate (10:1) to give a yellow powder (1.50 g, 24%, $R_f = 0.45$ in 90% ethyl acetate/petroleum ether).

m.p.: > 300 °C

^1H NMR (CDCl_3): 9.55 (d, 2H), 7.12 (s, 1H), 6.1 (s, 1H), 3.86 (d, 1H, $J = 10.4\text{Hz}$),

2.80 (m, 1H), 0.85 (d, 6H, $J = 7.4\text{Hz}$).

^{13}C NMR (CDCl_3): 153.1, 131.7, 125.7, 104.1, 43.3, 31.3, 22.2.

IR (cm^{-1}): 3382 br s, 2959 br m, 1619 s, 1499 s, 1441 m, 1301 m, 1157 m, 1069m, 838 m.

MS (LSIMS, positive): M^+ , 656; $M - \text{isopropyl}$, 613.

Elemental Analysis: ($\text{C}_{40}\text{H}_{48}\text{O}_8 \cdot \text{H}_2\text{O}$) found C 70.77%, H 7.76%; expected C 71.19%, H 7.47.

Tetra(*C*-dihexylmethyl)calix[4]resorcinarene (**22**)

Resorcinol (6.96 g, 63.1 mmol), α,α -dihexylacetaldehyde **20** (13.4 g, 63.1 mmol) and anhydrous ethanol (200 mL) were added into a 500 mL 3-neck round bottom flask with a stirring bar under a nitrogen atmosphere. The mixture was cooled to 0°C with an ice bath, and concentrated hydrochloric acid (32.8 g, 324 mmol) was added slowly via a syringe. The ice bath was replaced with a heating mantle, and the reaction solution was heated to 60°C for 72 hrs. Upon cooling, water (80 mL) was added to promote precipitation. The precipitate was dried under reduced pressure and purified by column chromatography with 50% ethyl acetate/petroleum ether to give pure compound **22** as a yellow-brown powder (15.2 g, 20%, $R_f = 0.7$ in 75% ethyl acetate/petroleum ether).

m.p.:134-136°C

$^1\text{H NMR}$ (CDCl_3): 9.46 (s, 2H), 7.16 (s, 1H), 6.04 (s, 1H), 3.96 (d, 1H), 3.52 (m, 1H), 1.64-2.52 (m, 4H), 1.16 (m, 16H), 0.78 (m, 6H).

$^{13}\text{C NMR}$ (CDCl_3): 152.1, 124.7, 123.8, 102.5, 64.8, 32.1, 30.2, 28.2, 25.5, 22.7, 21.0, 13.5

IR (cm^{-1}): 3290 br s, 2928 s, 1619 s, 1502 s, 1448 m, 1290 m, 843 w.

MS (LSIMS): M^+ , 1216; $M - [\text{CH}_3(\text{CH}_2)_5]_2\text{CH}$, 1033.

Elemental Analysis: ($\text{C}_{80}\text{H}_{128}\text{O}_8 \bullet 3\text{HCl}$) found C 73.10%, H 9.14%;

expected C 72.40%, H 9.95%.

2-Bromo-*N,N*-diethylacetamide (24)

Diethylamine (26.6 g, 356 mmol) was diluted in dry dichloromethane (250 mL) in a 500 mL 3-neck round bottom flask under a nitrogen atmosphere. The solution was cooled to -10 °C with an ice/NaCl bath and stirred. 2-Bromoacetyl bromide (32.6 g, 158 mmol) in dry dichloromethane (50 mL) was added dropwise into the flask from a constant addition funnel. After the addition, the reaction mixture was stirred for another 1 hr at -10 °C, and the mixture then warmed up to room temperature. After concentration the product was extracted with diethyl ether (300 mL). The ether extract was washed in turn with water (50 mL), saturated sodium bicarbonate (50 mL) and brine (50 mL), and dried over anhydrous magnesium sulfate and then evaporated under reduced pressure to give pure **24** as a colorless liquid (24.9 g, 81.2%; $R_f = 0.36$ in ethyl acetate).

$^1\text{H NMR}$ (CDCl_3): 3.75 (s, 2H), 3.29 (q, 4H, $J = 7.1\text{Hz}$), 1.16 (t, 3H, $J = 7.1\text{Hz}$),
1.04 (t, 3H, $J = 7.1\text{Hz}$).

$^{13}\text{C NMR}$ (CDCl_3): 165.9, 42.9, 40.5, 26.3, 14.3, 12.4.

IR (cm^{-1}): 2976 br s, 1644 s, 1454 s, 1228 m, 1094 m, 792 m, 609 m.

Tetra(*C*-isopropyl)calix[4]resorcinarene-3,5,10,12,17,19,24,26-octa- α -*N,N*-diethylacetamide (25)

Sodium hydride (500 mg of 60% in oil, 12.5 mmol) was washed with dry *n*-pentane (4 x 10 mL) and dried under a nitrogen atmosphere in a 3-neck 250 mL round bottom flask with a magnetic stirrer. Dry THF (100 mL) was added via a syringe

followed **22** (430 mg, 655 mmol). The mixture was stirred for 2 hrs, and then **24** (2.45 g, 12.5 mmol) in THF (30 mL) was added dropwise from a constant addition funnel. The mixture was heated to reflux for 24 hrs. After concentrated to 50 mL under reduced pressure, the residue was extracted into diethyl ether (300 mL). The ether layer was washed with water (3 x 50 mL) and brine (50 mL), and then dried over anhydrous magnesium sulfate and evaporated under reduced pressure. The crude product was purified by column chromatography with a gradient from 10 to 50% methanol/ethyl acetate to give pure compound **25** as a slightly yellow oil (600 mg, 59%, $R_f = 0.6$ in 15% methanol/ethyl acetate).

$^1\text{H NMR}$ (CDCl_3): 7.83 (s, 1H), 6.66 (s, 1H), 6.55 (s 1H), 6.45 (s 1H), 4.62 (d, 1H, $J = 10.2\text{Hz}$), 4.52 (m, 4H), 3.37 (m, 8H), 2.33 (m, 1H), 1.05 (m, 12H), 0.85 (d, 6H, $J = 7.3\text{Hz}$)

$^{13}\text{C NMR}$ (CDCl_3): 171.4, 158.6, 132.6, 130.1, 102.9, 73.4, 64.4, 45.6, 44.0, 36.0, 25.7, 18.4, 16.8.

IR (cm^{-1}): 2970 br s, 1644 s, 1584 w, 1466 br m, 1293 m, 1094 m, 797 w.

Elemental Analysis: ($\text{C}_{88}\text{H}_{136}\text{N}_8\text{O}_{16}$) found C 67.05%, H 8.77%, N 6.85%;
expected C 67.66%, H 8.78%, N 7.17%.

Tetra(*C*-dihexylmethyl)calix[4]resorcinarene-3,5,10,12,17,19,24,26-octa- α -*N,N*-diethyl-acetamide (26**)**

Sodium hydride (500 mg of 60% in oil, 12.5 mmol) was washed with dry *n*-pentane (4 x 10 mL) and dried under a nitrogen atmosphere in a 3-neck 250 mL round

bottom flask with a magnetic stirrer. Dry THF (100 mL) was added with a syringe followed by **22** (750 mg, 0.617 mmol). The mixture was stirred for 2 hrs, and then **24** (2.45 g, 12.5 mmol) in THF (30 mL) was added dropwise from a constant addition funnel. The mixture was heated to reflux for 24 hrs. The solvent was partially removed under reduced pressure and the product was extracted with diethyl ether (300 mL). The ether layer was washed with water (3 x 50 mL) and brine (50 mL), dried over anhydrous magnesium sulfate, and evaporated under reduced pressure. The crude product was purified by column chromatography with a gradient from 0 to 40% methanol/ethyl acetate to give pure **26** as a slightly yellow oil (1.00 g, 76%, $R_f = 0.5$ in 15% methanol/ethyl acetate).

$^1\text{H NMR}$ (CDCl_3): 6.80 (s, 1H), 6.30 (s, 1H), 4.59 (m, 1H), 4.40 (s, 4H), 3.86 (q, 1H, $J = 6.6\text{Hz}$), 3.22 (s, 8H), 1.74 (m, 2H), 1.51 (m, 2H), 0.97 (m, 28H), 0.74 (t, 6H, $J = 6.6\text{Hz}$).

$^{13}\text{C NMR}$ (CDCl_3): 167.8, 154.8, 127.5, 126.1, 99.1, 69.4, 65.0, 41.7, 40.4, 32.3, 30.3, 29.1, 24.7, 23.0, 21.3, 14.7, 14.5, 13.2.

IR (cm^{-1}): 2934 br s, 1643 s, 1580 w, 1502, br s, 1266 m, 796 w.

Elemental Analysis: ($\text{C}_{128}\text{H}_{216}\text{N}_8\text{O}_{16}\bullet\text{KCl}$) found C 69.00%, H 9.61%, N 5.78%; expected C 69.95%, H 9.91%, N 5.10%.

Tetra(C-hexyl)calix[4]resorcinarene-3,5,10,12,17,19,24,26-octa- α -*N,N*-diethylacetamide (27)

Sodium hydride (500 mg of 60% in oil, 12.5 mmol) was washed with dry *n*-pentane (4 x 10 mL) and dried under a nitrogen atmosphere in a 3-neck 250 mL round bottom flask with a magnetic stirrer. Dry THF (100 mL) was added via a syringe followed by the C-hexylcalix[4]resorcinarene (720 mg, 1.00 mmol).⁴⁹ The mixture was kept stirring for 2 hrs, and then **24** (2.45 g, 12.5 mmol) in THF (30 mL) was added dropwise from a constant addition funnel. The mixture was heated to reflux for 24 hrs. After concentrated to 50 mL, the reaction solution was mixed with diethyl ether (300 mL), and the diethyl ether layer was washed with water (3 x 50 mL) and brine (50 mL), and then dried over anhydrous magnesium sulfate and evaporated under reduced pressure. The crude material was purified by column chromatography with a gradient from 10 to 50% methanol/ethyl acetate to give pure **27** as slightly yellow oil (820 mg, 50%, $R_f = 0.4$ in 20% methanol/ethyl acetate).

$^1\text{H NMR}$ (CDCl_3): 6.81 (s, 1H), 6.46 (s, 1H), 4.62 (t, 1H, $J = 7.0\text{Hz}$), 4.17 (s, 4H), 3.44, (m, 8H), 1.82 (s, 2H), 1.21 (m, 12H), 1.09 (m, 12H), 0.85 (t, 3H, $J = 6.6\text{ Hz}$).

$^{13}\text{C NMR}$ (CDCl_3): 171.4, 158.5, 130.4, 130.2, 103.8, 73.1, 45.4, 44.0, 40.0, 39.3, 36.0, 34.0, 33.4, 32.3, 26.6, 18.3, 18.1, 16.8.

IR (cm^{-1}): 2934 br s, 1642 s, 1584 m, 1467 br s, 1296 s, 1101 s, 796 m.

Elemental Analysis: ($\text{C}_{104}\text{H}_{168}\text{N}_8\text{O}_{16}$) found C 69.66%, H 9.72%, N 6.12%,
expected C 69.92%, H 9.84%, N 6.27%.

**Tetra(*C*-methyl)calix[4]resorcinarene-3,5,10,12,17,19,24,26-octa- α -*N,N*-
diethylacetamide (28)**

Sodium hydride (1.18 g of 60% in oil, 24.9 mmol) was washed with dry *n*-pentane (4 x 10 mL) and dried under a nitrogen atmosphere in a 3-neck 250 mL round bottom flask with a magnetic stirrer. Dry THF (100 mL) was added via a syringe followed by the *C*-methylcalix[4]resorcinarene⁴⁹ (550 mg, 1.0 mmol). The mixture was stirred for 2 hrs, and then **24** (5.72 g, 29.5 mmol) in THF (30 mL) was added dropwise from a constant addition funnel. The mixture was heated to reflux for 24 hrs. After concentration the product was extracted into diethyl ether (300 mL), and the ether extract was washed with water (3 x 50 mL) and brine (50 mL), dried over anhydrous magnesium sulfate, and evaporated under reduced pressure. The crude product was purified by column chromatography with a gradient from 0 to 50% methanol/ethyl acetate to give pure **28** as a slightly yellow oil (707 mg, 42%, $R_f = 0.5$ in 50% methanol/ethyl acetate).

¹H NMR (CDCl₃): 6.36 (s, 2H), 4.60 (q, 1H, $J = 7.0\text{Hz}$), 4.35 (s, 4H), 3.26 (d, 8H, $J = 6.6\text{Hz}$), 1.36 (d, 3H, $J = 7.1\text{Hz}$), 1.01 (m, 12H).

¹³C NMR (CDCl₃): 171.6, 158.4, 131.8, 129.7, 103.0, 73.0, 45.4, 44.0, 34.6, 24.2, 18.3, 16.8.

IR (cm⁻¹): 2973 br m, 1642 s, 1586 w, 1499 m, 1267 m, 1119 m, 799 w.

MS: M^+ , 1448.

Elemental Analysis: ($C_{80}H_{120}N_8O_{16} \bullet H_2O$) found C 65.55%, H 8.56%, N 7.40%,
expected C 65.46%, H 8.38%, N 7.63%;

**Tetra(*C*-dihexylmethyl)calix[4]resorcinarene-3,5,10,12,17,19,24,26-octa-methyl
acetate (29)**

Sodium hydride (400 mg of 60% in oil, 10.0 mmol) was washed with dry *n*-pentane (4 x 10 mL) and dried under a nitrogen atmosphere in a 3-neck 250 mL round bottom flask with a magnetic stirrer. Dry THF (100 mL) was added with a syringe followed **22** (750 mg, 0.617 mmol). The mixture was stirred for 2 hrs, and then methyl bromoacetate (1.53 g, 10.0 mmol) in THF (30 mL) was added dropwise from a constant addition funnel. The mixture was heated at reflux for 24 hrs. After concentration, the reaction solution was extracted with diethyl ether (300 mL). The ether layer was washed with water (3 x 50 mL) and brine (50 mL), and then dried over anhydrous magnesium sulfate and evaporated under reduced pressure. The crude product was purified by column chromatography with a gradient by 50% ethyl acetate/petroleum ether, 100% ethyl acetate, 1% MeOH/ethyl acetate and 5% MeOH/ethyl acetate to give pure **29**. Two isomers of **29** were obtained as brown oil (200 mg, 18%, $R_{f1} = 0.7$ in 75% ethyl acetate/petroleum ether, $R_{f2} = 0.5$ in 5% methanol/ethyl acetate).

1H NMR ($CDCl_3$): 7.1 (m, 1H), 6.2 (m, 1H), 4.48 (m, 4H), 4.31 (d, 1H), 4.04 (s, 1H), 3.70 (m, 6H), 1.64 - 2.12 (m, 4H), 1.24 (m, 16H), 0.87 (m, 6H).

^{13}C NMR (CDCl_3): 172.7, 156.7, 129.2, 127.5, 105.1, 69.8, 68.4, 56.6, 44.0, 40.2, 35.9, 33.6, 28.6, 24.9, 18.0.

IR (cm^{-1}): 2930 br s, 1755 s, 1613 m, 1496 s, 1439 m, 1224 br m, 723 w.

Elemental Analysis: ($\text{C}_{104}\text{H}_{160}\text{O}_{24}$) found C 69.61%, H 8.65; expected C 69.64%, H 8.93%.

3.3 Preparation of Langmuir films and Langmuir-Blodgett Films

The solvents used to prepare the spreading solutions were UV-grade chloroform and toluene and HPLC-grade methanol from Aldrich. Silver nitrate (assay 99.98%) from Aldrich was used without further purification. The resorcinarenes or their derivatives were prepared in concentration of 2×10^{-4} M in 10% methanol/chloroform or 10% methanol/toluene solutions. Langmuir films of these compounds were spread via a 100- μL syringe onto a Lauda Langmuir Film Balance equipped with a Lauda Fl-1 electronically controlled dipping device. The subphase was double-distilled water which was passed through a Milli-Q Plus filtration system, with a final resistivity of 18.2 $\text{M}\Omega\text{cm}$ or solution of 2×10^{-4} M AgNO_3 in Milli-Q filtered water. The monolayers were compressed at a rate of 2 mm/min after a waiting period of 30 min for the solvent evaporation and/or interaction between the resorcinarenes and the subphase. All π -A isotherms were recorded at 15 or 25°C ($\pm 0.1^\circ\text{C}$) controlled by Lauda temperature controller. The Langmuir-Blodgett films were transferred onto quartz in the vertical mode at a deposition rate of 2 mm/s. The surface pressure was kept constant during the transfer process by using the Lauda Fl-1 electronically controlled dipping device.

4. REFERENCES

1. Lehn, J.-M. *Science*, **1985**, *227*, 849-856.
2. Lehn, J.-M. *Pure Appl. Chem.*, **1980**, *52*, 2441-2459.
3. Cram, D. J. *Angew. Chem. Intl. Ed. Engl.* **1988**, *27*, 1009-1020.
4. Vögtle, F. *Supramolecular Chemistry*; Wiley: **1991**, pp 7.
5. Pedersen, C. J. *J. Am. Chem. Soc.* **1967**, *89*, 7017-7035.
6. Dietrich, B.; Lehn, J.-M.; Sauvage, J. P. *Tetrahedron Lett.* **1969**, 2885-2889.
7. Cram, D. J.; Cram, J. M. *Science* **1974**, *183*, 803-809.
8. Lehn, J. M. *Angew. Chem. Intl. Ed. Engl.* **1988**, *27*, 89-112.
9. Pedersen, C. J. *Angew. Chem. Intl. Ed. Engl.* **1988**, *27*, 1021-1027.
10. Pedersen, C. J. *Angew. Chem. Intl. Ed. Engl.* **1988**, *27*, 2495-2496.
11. Dietrich, B.; Lehn, J. M.; Sauvage, J. P. *Tetrahedron Lett.* **1969**, 2889-2892.
12. Trueblood, K. N.; Knobler, C. B.; Maverick, E.; Helgeson, R. C.; Brown, S. B.; Cram, D. J. *J. Am. Chem. Soc.* **1981**, *103*, 5594-5596.
13. Cram, D. J.; Lein, G. M.; *J. Am. Chem. Soc.* **1985**, *107*, 3657-3668.
14. Vögtle, F. *Supramolecular Chemistry*; Wiley: **1991**, pp 284.
15. Hoffmann, H.; Ebert, G. *Angew. Chem. Intl. Ed. Engl.* **1988**, *27*, 902-905.
16. Thoden van Velzen, E. U.; Engberson, J. F. J.; de Lange, P. J.; Mahy, J. W. G.; Reinhoudt, D. N. *J. Am. Chem. Soc.*, **1995**, *117*, 6853-6862.
17. Baeyer, A. *Ber.*, **1872**, *5*, 1094-1101.
18. Gutsche, C. D. *Calixarene: Monographs in Supramolecular Chemistry*, Stoddart, J. F., Ed., Royal Society of Chemistry: Cambridge, **1989**, pp 88.

19. Lederer, L. *J. Prakt. Chemie*, **1894**, *50*, 23.
20. Manasse, O. *Ber.*, **1894**, *27*, 2409.
21. Baekeland, L. H. US patent 942699, October, **1908**.
22. Neiderl, J. B.; Vogel, H. J. *J. Am. Chem. Soc.*, **1940**, *62*, 2512.
23. Zinke, A.; Ziegler, E. *Ber.*, **1941**, *B74*, 1729.
24. Zinke, A.; Ziegler, E. *Ber.*, **1944**, *77*, 264.
25. Zinke, A.; Kretz, R.; Leggewie, E.; Hössinger, K. *Monatsh. Chem.*, **1952**, *83*, 1213-1227.
26. Cornforth, J. W.; Morgan, E. D.; Potts, K. T.; Rees, R. J. W. *Tetrahedron*, **1973**, *29*, 1659-1667.
27. Gutsche, C. D.; Iqbal, M.; Stewart, D. *J. Org. Chem.*, **1986**, *51*, 742-745.
28. Gutsche, C. D.; Dhawan, B.; No, K. H.; Muthukrishnan, R. *J. Am. Chem. Soc.*, **1981**, *103*, 3782-3792.
29. Munch, J. H.; Gutsche, C. D. *Org. Syn.*, **1989**, *68*, 243-245.
30. Weinelt, F.; Shneider, H. J. *J. Org. Chem.*, **1991**, *56*, 5527-5535.
31. Högberg, A. G. S. *J. Am. Chem. Soc.*, **1980**, *102*, 6046-6065.
32. Högberg, A. G. S. *J. Org. Chem.*, **1980**, *45*, 4498-4500.
33. Cram, D. J.; Karbach, S.; Kim, H. E.; Knobler, C. B.; Maverick, E. F.; Ericson, J. L.; Helgeson, R. C. *J. Am. Chem. Soc.*, **1988**, *110*, 2229-2237.
34. Gutsche, C. D. *Calixarenes*, Royal Society of Chemistry:Cambridge, **1989**, pp 90.
35. Kämmerer, H.; Happel, G.; Caesar, F. *Makromol. Chem.*, **1972**, *162*, 179-197.
36. Gutsche, C. D.; Dhawan, B.; Levine, J. A.; No, K. H.; Bauer, L. J. *Talanta*, **1983**, *39*, 409-412.
37. Gutsche, C. D.; Bauer, L. J. *J. Am. Chem. Soc.*, **1985**, *107*, 6052-6059.
38. Andreeti, G. D.; Ungaro, R.; Pochini, A. *J. Chem. Soc., Chem. Commun.* **1979**, 1005-1007.
39. Andreeti, G. D.; Pochini, A.; Ungaro, R. *J. Chem. Soc., Perkin II*, **1983**, 1773-1779.

40. Erdtman, H.; Högberg, A. G. S.; Abrahamsson, S.; Nilsson, B. *Tetrahedron Lett.*, **1968**, 1679-1682.
41. Palmer, K. J.; Wong, R. Y.; Jurd, L.; Stevens, K. *Acta Cryst.*, **1976**, *B32*, 847-849.
42. Högberg, A. G. S. *J. Org. Chem.*, **1980**, *45*, 4498-4500.
43. Tunstad, L. M.; Tucker, J. A.; Dalcanadle, E.; Weiser, J.; Bryant, J. A.; Sherman, J. C.; Helgeson, R. C.; Knobler, C. B.; Cram, D. J. *J. Org. Chem.* **1989**, *54*, 1305-1312.
44. Aoyama, Y.; Tanaka, Y.; Sugahara, S.; *J. Am. Chem. Soc.*, **1989**, *111*, 5397-5404.
45. Konoshi, H.; Morikawa, O. *J. Chem. Soc., Chem. Commun.*, **1993**, 34-35.
46. Fransen, J. R.; Dutton, P. L. *Can. J. Chem.* **1995**, *73*, 2217-2223.
47. Moran, J. R.; Karbach, S.; Cram, D. J. *J. Am. Chem. Soc.* **1982**, *104*, 5826-5828.
48. Cram, D. J.; Stewart, K. D.; Goldberg, I.; Trueblood, K. N. *J. Am. Chem. Soc.*, **1985**, *107*, 2574-2576.
49. Cram, D. J.; Karbach, S.; Kim, Y. H.; Baczynskyj, L.; Marti, K.; Sampson, R. M.; Kalleymeyn, G. M. *J. Am. Chem. Soc.*, **1988**, *110*, 2554-2560.
50. Sherman, J. C.; Knobler, C. B.; Cram, D. J. *J. Am. Chem. Soc.*, **1991**, *113*, 2194-2204.
51. Cram, D. J.; Tanner, M. E.; Knobler, C. B. *J. Am. Chem. Soc.*, **1991**, *113*, 7717-7727.
52. Cram, D. J.; Tanner, M. E.; Thomas, R. *Angew. Chem. Intl. Ed. Engl.*, **1991**, *30*, 1024-1027.
53. Aoyama, Y.; Tanaka, Y.; Toi, H.; Ogoshi, H. *J. Am. Chem. Soc.*, **1988**, *110*, 634-635.
54. Kikuchi, Y.; Kato, Y.; Tanaka, Y.; Toi, H.; Aoyama, Y. *J. Am. Chem. Soc.*, **1991**, *113*, 1349-1354.
55. Tanaka, Y.; Ubukata, Y.; Aoyama, Y. *Chem. Lett.*, **1989**, 1905-1908.
56. Tanaka, Y.; Kato, Y.; Aoyama, Y. *J. Am. Chem. Soc.*, **1990**, *112*, 2807-2808.
57. Kikuchi, Y.; Kobayashi, K.; Aoyama, Y. *J. Am. Chem. Soc.*, **1992**, *114*, 1351-1358.

58. Kobayashi, K.; Asakawa, Y.; Kikuchi, Y.; Toi, H.; Aoyama, Y. *J. Am. Chem. Soc.*, **1993**, *115*, 2648-2654.
59. Schneider, H. J.; Kramer, R.; Simova, S.; Schneider, U. *J. Am. Chem. Soc.*, **1988**, *110*, 6442-6448.
60. Schneider, H. J.; Güttes, D.; Schneider, U. *J. Am. Chem. Soc.*, **1988**, *110*, 6449-6454.
61. Koide, Y.; Oka, T.; Imamura, A.; Shosenji, K.; Yamada, K. *Bull. Chem. Soc. Jpn.*, **1993**, *66*, 2137-2142.
62. Dutton, P. L.; Conte, L. *Langmuir*, in press.
63. Langmuir, I. *J. Am. Chem. Soc.*, **1917**, *39*, 1848.
64. Blodgett, K. B. *Trans. Faraday Soc.*, **1920**, *57*, 62.
65. Blodgett, K. B. *J. Am. Chem. Soc.*, **1935**, *57*, 1007-1012.
66. Roberts, G. (Ed.) *Langmuir-Blodgett Films*, Plenum: New York, **1990**, pp 21.
67. Harkins, W. D.; Young, T. F.; Boyd, E. *J. Chem. Phys.*, **1940**, *8*, 954-965.
68. Roberts, G. (Ed.) *Langmuir-Blodgett Films*, Plenum, New York, **1990**, pp 27.
69. Ter Minassian Saraga, L. *J. Chem. Phys.*, **1955**, *52*, 181.
70. Jr. Gaines, G. L. *Insoluble Monolayers at Liquid-Gas Interfaces*, Wiley: New York, **1966**.
71. Delaney, P. A.; Johnstone, R. A. W.; Eyres, B. L.; Hann, R. A.; McGrath, I.; Ledwith, A. *Thin Solid Films*, **1985**, *123*, 353-360.
72. Stewart, F. H. C. *Aust. J. Chem.*, **1961**, *14*, 57-63.
73. Vincett, P. S.; Barlow, W. A. *Thin Solid Films*, **1980**, *71*, 305-326.
74. Steven, J. H.; Hann, R. A.; Barlow, W. A.; Laird, T. *Thin Solid Films*, **1983**, *99*, 71-79.
75. Vicens, J.; Böhmer, V. *Calixarenes: A Versatile Class of Macrocyclic Compounds*, Kulwer, **1993**, *3*, pp 237.
76. Ishikawa, Y.; Kunitake, T.; Matsuda, T.; Otsuka, T.; Shikai, S. *J. Chem. Soc., Chem. Commun.*, **1989**, 736-738.

77. Sakaki, T.; Harada, T.; Deng, G.; Kawabata, H.; Kawahara, Y.; Shinkai, S. *J. Include. Phenom. Mol. Recogn.*, **1992**, *14*, 285.
78. Komiyama, M.; Isaka, K.; Shikai, S. *Chem. Lett.*, **1991**, 937-940.
79. Sato, N.; Shinkai, S. *Chem. Soc. Perkin Trans. 2*, **1993**, 621-624.
80. Arduini, A.; Pochini, S.; Reverberi, S.; Ungaro, R.; Andreetti, G. D.; Ugozzoli, F. *Tetrahedron*, **1986**, *42*, 2089-2100.
81. Mckervery, M. A.; Seward, E. W.; Ferguson, G.; Ruhl, B. L. *J. Org. Chem.*, **1986**, *51*, 3581-3584.
82. Chang, S. K.; Cho, I. *J. Chem. Soc., Perkin Trans. 1*, **1986**, 211-214.
83. Dei, L.; Casnati, A.; Lo Nostro, P.; Baglioni, P. *Langmuir*, **1995**, *11*, 1268-1272.
84. Moreira, W. C.; Dutton, P. J.; Aroca, R. *Langmuir*, **1995**, *10*, 4148-4152.
85. Moreira, W. C.; Dutton, P. J.; Aroca, R. *Langmuir*, **1995**, *11*, 3137-3144.
86. Schierbaum, K. D.; Weiss, T.; Thoden van Velzen, E. U.; Engbersen, J. F. J.; Reinhoudt, D. N.; Gopel, W. *Science* **1994**, *265*, 1413-1415.
87. Huisman, B.-H.; Thoden, van Velzen, E. U.; van Veggel, F. C. J. M.; Engbersen, J. F. J.; Reinhoudt, D. N. *Tetrahedron Lett.* **1995**, *36*, 3273-3276.
88. Huisman, B.-H.; Rudlkevich, D. M.; van Veggel, F. C. J. M.; Reinhoudt, D. N. *J. Am. Chem. Soc.*, **1996**, *118*, 3523-3524.
89. Erdtman, H.; Högberg, S.; Abrahamsson, S.; Nilsson, B. *Tetrahedron Lett.*, **1968**, 1679-1682.
90. Moore, S. S.; Tarnowski, T. L.; Newcomb, M.; Cram, D. J. *J. Am. Chem. Soc.*, **1977**, *99*, 6398-6405.
91. Kluge, A. F.; Cloudsdale, I. S. *J. Org. Chem.*, **1979**, *44*, 4847-4852.
92. Pavia, D. L.; Lampman, G. M.; Jr. Kriz, G. S. *Introduction to Spectroscopy*, Saunders, **1979**, pp 47.
93. March, J. *Advanced Organic Chemistry*, Wiley: **1992**, pp 1346.
94. Kem, K. M.; Nguyen, N. V.; Cross, D. J. *J. Org. Chem.*, **1981**, *46*, 5188-5192.
95. McKervery, M. A.; Seward, E. M.; Ferguson, G.; Ruhl, B.; Harris, S. J. *J. Chem. Soc. Chem. Commun.*, **1985**, 388-390.

96. Fransen, J. R. Master's degree Thesis, pp 85.
97. Lambert, J. B.; Shurvell, H. F.; Lighter, D.; Cooks, R. G. *Introduction to Organic Spectroscopy*, Macmillian, 1987, pp 454.
98. Silverstein, R. M.; Bassler, G. C.; Morrill, T. C. *Spectrometric Identification of Organic Compounds*, 5th Edition, Wiley, 1991, pp 419.
99. Lin, J. D.; Popov, A. I. *J. Am. Chem. Soc.*, 1981, 103, 3773-3777.
100. Takai, Y.; Okumura, Y.; Tanaka, T.; Sawada, M.; Takahashi, S.; Shiro, M.; Kawamura, M.; Uchiyama, T. *J. Org. Chem.*, 1994, 59, 2967-2975.
101. Tsukube, H.; Sohmiya, H. *J. Org. Chem.*, 1991, 56, 875-878.
102. de Boer, J. A. A.; Reinhoudt, D. N. *J. Am. Chem. Soc.*, 1985, 107, 5347-8351.
103. Bradshaw, J. S.; Maas, G. E.; Lanb, J. D.; Izatt, R. M.; Christensen, J. J. *J. Am. Chem. Soc.*, 1980, 102, 467-450.
104. Live, D.; Chan, S. I. *J. Am. Chem. Soc.*, 1976, 98, 3769-3772.
105. Groenen, L. C.; Steinwender, E.; Lutz, B. T. G.; van der Mass, J. H.; Reinhoudt, D. N. *J. Chem. Soc. Perkin Trans. 2*, 1992, 1893-1898.

VITA AUCTORIS

NAME Yong Chun Chen

PLACE OF BIRTH Fujian, China

BIRTH DATE January 15, 1963

EDUCATION Xiamen University, Xiamen, Fujian, China
B.Sc. in Chemistry
1981 - 1985

University of Sherbrooke, Sherbrooke, Quebec, Canada
M.A.Sc. in Chemical Engineering
1993 - 1995

University of Windsor, Windsor, Ontario, Canada
M.Sc. in Chemistry
1995 - 1999

CARRERS Beijing Research Institute of Chemical Industry, Beijing, China
Chemical Engineer
1985 - 1992

Ferndale Laboratories, Inc., Ferndale, Michigan, USA
Scientist
1998 - present